



A First Look at the Gravettian Open-Air Site Ollersdorf-Heidenberg (Austria): Recent Fieldwork and First Results on Stratigraphy, Chronology, Organic Preservation and Combustion Activity

Marjolein D. Bosch^{1,2,3} · Stéphane Pirson^{4,5} · Freddy Damblon⁶ · Margarita Jambrina-Enrriquez^{7,8} · Carolina Mallol^{7,9} · Alexander Pryor¹⁰ · William Chase Murphree¹¹ · Bence T. Viola¹² · Walpurga Antl-Weiser² · Philip R. Nigst^{3,13}

Accepted: 24 January 2025
© The Author(s) 2025

Abstract

The Middle Danube region is a key area for understanding Upper Palaeolithic hunter-gatherer behaviours in a climatic context due to its long loess–palaeosol sequences and rich archaeological record spanning from the onset of the Upper Palaeolithic to the Last Glacial Maximum and beyond. Recently, new approaches focusing on high-resolution studies of the stratigraphy, geoarchaeological studies at microscopic scale and investigations of organic matter at molecular scale (biomarker analyses) have shown great new insights in human behaviour. Many sites in the Middle Danube region have been excavated a long time ago without opportunity to apply such approaches. The aim of this paper is to introduce Ollersdorf-Heidenberg, a loess open-air site. The site is located ~26 km northeast of Vienna close to the Morava River valley and preserves several Upper Palaeolithic archaeological horizons. The site has been known since a pipeline construction in 1998. Here, we report the first results of new research at the site including new excavations in two trenches. We describe and analyse the stratigraphy, present a first radiocarbon date, describe and analyse lithic and faunal collections, and assess potential in situ combustion activity and the preservation of organic matter. Research at the site is ongoing, but our preliminary results let us suggest good preservation of organic matter and, hence, Ollersdorf-Heidenberg has a remarkable potential for providing valuable insights in past hunter-gatherer behaviours at the climatic downturn towards the Last Glacial Maximum.

Keywords Upper Palaeolithic · Gravettian · Central Europe · Hunter-Gatherers · Open-air site

Introduction

The time period from around 35 to 23 thousand years ago (kya)—leading up to and including the earlier part of the Last Glacial Maximum—is characterised by a general slow trend to colder and especially more arid environmental conditions, which is evident from the high-resolution climate records of both the Greenland ice-cores (e.g. Rasmussen et al., 2014) and the loess–palaeosol sequences of continental Eurasia (e.g. Haesaerts et al., 2009, 2010, 2016). This period of climatic downturn coincides with the European Mid-Upper Palaeolithic, i.e. Gravettian, from around 35 to 24 kya. From 35 kya onwards, we can observe several major changes in the archaeological record related to shifts in human behaviour. These changes include more permanent site infrastructure,

longer site occupation phases, increased raw material transfer distances, first use of plants as food in the European Palaeolithic documented through plant macrofossils, first evidence of the use of pestle grinders for plant processing in the European Palaeolithic, first ceramic technology and increased evidence for symbolically imbued objects (e.g. Svoboda et al., 1996; Gamble, 1999; Verpoorte, 2001; Revedin et al., 2010; Moreau et al., 2021; Pryor et al., 2013). In eastern Central Europe, these observations are typical for the Early (~35–31 kya; e.g. Moreau, 2009) and Middle Gravettian (or Pavlovian; ~31/30–29 kya; e.g. Svoboda, 2016), while during the Late Gravettian (~30/29–24 kya; e.g. Wilczyński, 2016; Lengyel & Wilczyński, 2018) small/ephemeral sites prevail, with less investment in site infrastructure and more specialised hunting strategies (e.g. Svoboda et al., 1996; Verpoorte, 2004; Wilczyński et al., 2020a).

One of the centres for the above observations and related debates on human behaviour has been the Middle

Extended author information available on the last page of the article

Danube region and its abundant Gravettian localities, which include rich and well-known sites like those of the site complexes of Willendorf (e.g. Felgenhauer, 1959; Haesaerts et al., 1996; Nigst et al., 2014), Pavlov-Dolní Věstonice (e.g. Svoboda et al., 1996, 2016; Svoboda, 2005, 2015, 2019), Předmostí (e.g. Svoboda et al., 1994), Milovice (e.g. Oliva, 1988, 2009; Svoboda et al., 2011), Moravany (e.g. Hromada & Kozłowski, 1995; Kozłowski, 1998; Polanská & Hromadová, 2015), Krakow-Spadzista Street (e.g. Wilczyński, 2016; Wojtal et al., 2015), Krems (e.g. Einwögerer, 2000; Neugebauer-Maresch, 2008; Simon et al., 2014) and Grub-Kranawetberg (e.g. Antl & Bosch, 2015; Antl-Weiser et al., 2010; Nigst & Antl-Weiser, 2012). However, there are also many smaller sites known from both surface collections as well as excavations (e.g. Skrdla, 2005).

Many of the Gravettian sites in the Middle Danube region have yielded collections including abundant charcoal remains (e.g. Beresford-Jones et al., 2010, 2011; Cichoński et al., 2014; Damblon et al., 1996; Haesaerts et al., 2010; Nigst et al., 2014). At Dolní Věstonice II, studies have shown the presence of plant macroremains providing interesting insights in Gravettian hunter-gatherer plant use and diet (Mason et al., 1994; Pryor et al., 2013). Some of the larger sites show evidence of intense and potentially repeated occupations, e.g. at Willendorf II, Pavlov I, Dolní Věstonice I and II, Grub-Kranawetberg I and Krems-Wachtberg (Antl-Weiser et al., 2010; Felgenhauer, 1959; Nigst et al., 2014; Nigst & Antl-Weiser, 2012; Simon et al., 2014; Svoboda, 2005; Svoboda et al., 1996, 1999, 2016). At Grub-Kranawetberg I, human presence resulted in the formation of anthrosols as a consequence of anthropogenic input of mineral and organic matter (Schilt et al., 2017). However, many of the sites have been excavated a long time ago and, hence, the application of techniques to extract information on organic matter—either through micromorphological or biomarker analysis—has been limited. It is essential to collect new data on the Mid-Upper Palaeolithic hunter-gatherer behaviours especially in relation to plant use and human occupation intensity to better understand variation in the Gravettian—and especially Late Gravettian—archaeological context.

The opportunity to test a site in the Middle Danube region for such investigations arose recently at the site Ollersdorf-Heidenberg in Austria, located NE of Vienna (Fig. 1a, b). The site is known since in 1998 and 2007 pipeline construction discovered and sadly also partly destroyed the site (Antl, 1998, 2007; Antl-Weiser, 2008). Those 1998 and 2007 rescue excavations documented two archaeological layers with evidence of combustion activity, rich charcoal and faunal assemblages as well as a lithic collection including unretouched bladelets and burins (Antl-Weiser, 2008). Between 2017 and 2022, we conducted three fieldwork campaigns (interrupted by the COVID-19 pandemic) at the site.

In this paper, we present the first fieldwork activity at the site focused at research rather than rescue archaeology under time constraints. We present first results including a description of the sequence, a first radiocarbon date, an overview of the lithic and faunal collections, and an assessment of both the preservation of organic matter and potential in situ combustion activity.

Ollersdorf-Heidenberg: Site Location, Research History and New Fieldwork

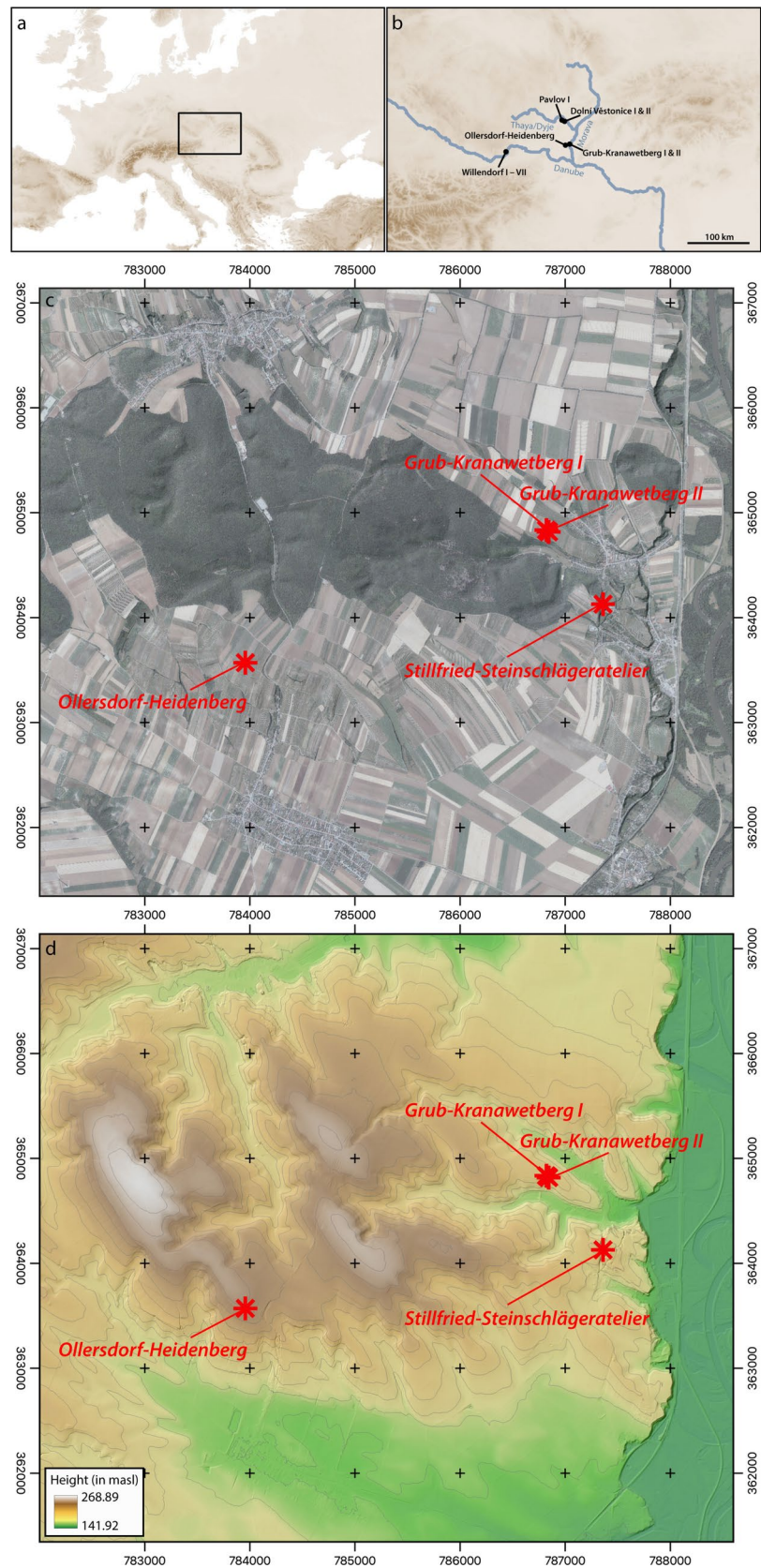
Ollersdorf-Heidenberg (48° 24' 34.0" N, 16° 47' 26.75" E) is located about 26 km to the northeast of Vienna (Fig. 1a, b). It is situated on the southern fringes of the low rolling hills of the so-called Weinviertel area. The site, located on top of a hill at an elevation of 237 masl, has views to the south over the Marchfeld plain that is delimited by the Danube to the south and by the Morava to the east. Nowadays, the closest (~4.5 km distance) river is the Morava, a tributary to the Danube. The top sedimentary deposits of the hill on which Ollersdorf-Heidenberg is located are formed by loess-like sediments. Their thickness remains currently unknown, but can be estimated to at least 4 m based on drilling prospecting (by hand auger) as part of our first fieldwork campaign in 2017 (Antl-Weiser et al., 2019).

In the surrounding area and less than 4 km distant three stratified Upper Palaeolithic sites of roughly similar chronostratigraphic position, Grub-Kranawetberg I (e.g. Antl-Weiser, 2010), Grub-Kranawetberg II (Bosch et al., in press a, in press b) and Stillfried-Steinschlägeratelier (Felgenhauer, 1980) are known (Fig. 1c, d). A further 10 Upper Palaeolithic sites are known by surface collections that yielded Upper Palaeolithic (mainly Gravettian but also Aurignacian) lithic artefacts and faunal remains (e.g. Antl-Weiser, 2008; Nigst et al., 2024).

The site of Ollersdorf-Heidenberg was unknown up to 1998 when oil pipeline construction led to its discovery (Antl, 1998; Antl-Weiser, 2008). At least two Gravettian archaeological layers separated by sterile loess deposits were observed and again recognised in 2007 when the same company placed a gas pipeline through the site (Fig. 2a–c). Both pipeline trenches provided abundant archaeological remains including faunal remains (among others, horse, reindeer and mammoth) showing well-preserved cortical surfaces as well as a perforated *Glycymeris* sp. shell, and lithic artefacts including unretouched bladelets (e.g. Antl, 1998, 2007; Antl-Weiser, 2008).

In both pipeline trenches, abundant and well-preserved charcoal could be observed along the exposed sections. From the lower and richer archaeological horizon in the 1998 pipeline trench, charcoal has been dated to 25,450 ± 90 ka uncal. BP (VERA-366, charcoal; 30,006–29,322 cal BP [95.4%

Fig. 1 Location of Ollersdorf-Heidenberg. Map of Europe (a) and Middle Danube region (b) showing the location of Ollersdorf-Heidenberg and other sites mentioned in the text. Map showing the location of the sites Ollersdorf-Heidenberg, Grub-Kranawetberg I and II, and Stillfried-Steinschlägeratelier on top of an orthophoto (c) and a digital terrain model (d). Basemap and rivers in (a) and (b); HYDRO1K dataset from U.S. Geological Survey Earth Resources Observation and Science Center, <https://doi.org/https://doi.org/10.5066/F77P8WN0>; coordinate reference system for (a) and (b): WGS84/UTM grid system [northern hemisphere] [EPSG code 32600]. Areal images/orthophotos in (c): Land Niederösterreich; elevation, hillshade and 1-m-contour lines calculated from a digital terrain model with 1-m resolution: Land Niederösterreich; coordinate reference system for (c) and (d): MGI/Austria GK M34 [EPSG code 31259]. GIS and graphic: P. R. Nigst



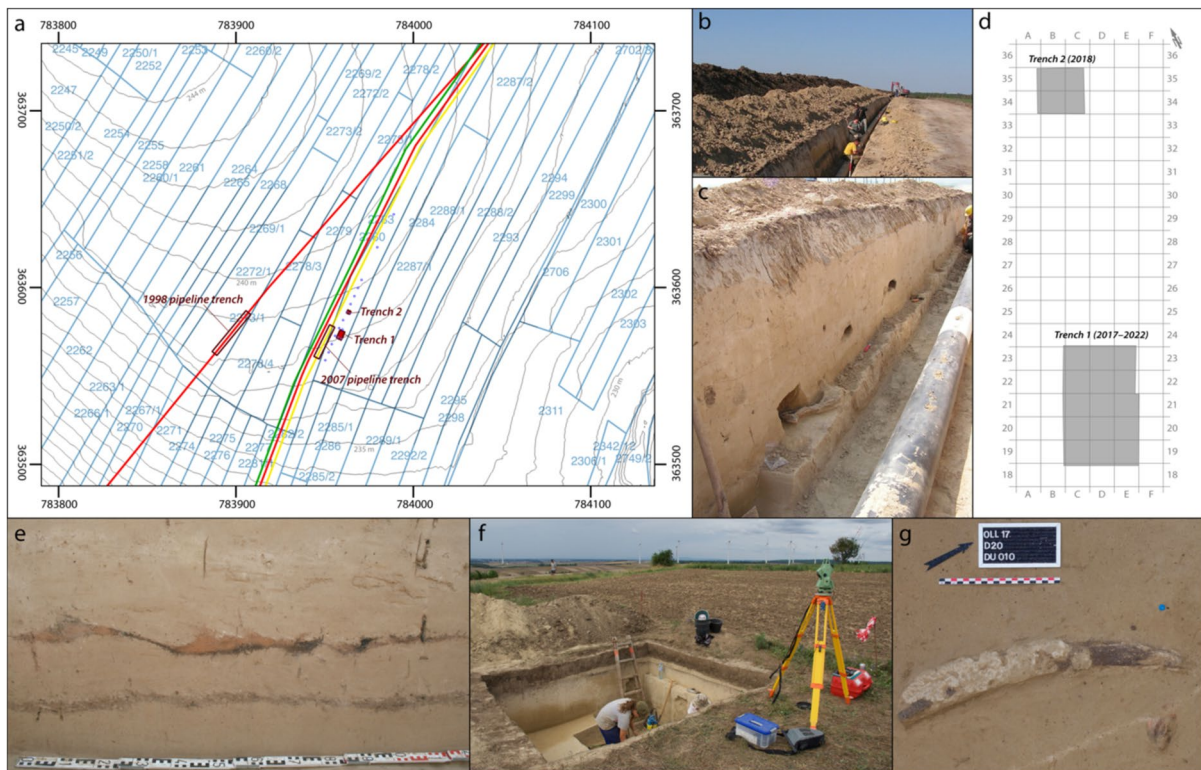


Fig. 2 a) Cadastral map with location of 1998 and 2007 pipeline trenches, 2017 borings (blue circles) and Trenches 1 and 2 (excavation 2017–2022) in relation to oil pipelines (red; 1998 and 2009), gas pipeline (yellow; 2007) and district heating line (green; unknown year) (Cadastral map [Digitale Katastralmappe]: Bundesamt für Eich- und Vermessungswesen, Vienna. One-meter-contour lines calculated from a digital terrain model with 1-m resolution [source: Land Niederösterreich]; Coordinate reference system: MGI/Austria GK M34 [EPSG code 31259]) (GIS and graphic: P. R. Nigst). (b) 2007 pipe-

line trench during excavation (photo: H. Preisl). (c) 2007 pipeline trench during excavation, large faunal remains visible in foreground (photo: H. Preisl). (d) Map of the 2017–2022 excavations in Trenches 1 and 2 in the local excavation grid (map: Ph. R. Nigst). (e) Section photograph of the 2007 pipeline trench showing the two archaeological horizons (photo: W. Antl-Weiser). (f) 2018 excavation in Trench 1 (photo: P. R. Nigst). (g) Rib fragment of ungulate size class 3–4 animal during the excavation 2017 in Trench 1, SU C4a, AH Anna (photo: P. R. Nigst)

probability]; Antl-Weiser, 2008; Antl-Weiser et al., 2010). In the 2007 pipeline trench, the upper archaeological horizon showed abundant evidence of reddish-coloured sediment (Antl-Weiser, 2008) (Fig. 2e) congruent with combustion activity (this is based on macroscopic observations, no geoarchaeological or micromorphological assessment was done at the time).

In 2017, some of us (MDB, WAW and PRN) decided to go back to the site to conduct borings and test-excavations (Fig. 2a, d, f, g) exploring the still accessible parts of the site east of the pipelines. Specifically, we were interested in (i) assessing the organic preservation at the site, (ii) testing the impact of combustion activities at the site and (iii) testing the potential of the site for future work focusing on organic matter and plant macroremains.

During our fieldwork in 2017, 2018 and 2022, we had to keep a minimum security distance of 5 m to the two oil pipelines, as well as one gas pipeline and one district heating pipeline (when the latter one was put in the ground is not known to us). In 2017, we started our fieldwork with trying to locate the archaeological layers observed in the previous

fieldwork constrained by (i) respecting the minimum distance of 5 m east of the 2007 pipeline and (ii) crop harvest time on the involved cadastral parcels. Therefore, all our fieldwork was limited to parcel 2283 of KG Ollersdorf (MG Angern an der March, VB Gänserndorf). Our 2017 fieldwork started with a boring campaign, which was conducted by using an Edelman hand auger and in total 17 borings (Fig. 2a – blue circles) were made (Antl-Weiser et al., 2019). Based on brownish-coloured sediment of 1–3 cm thickness in six borings and light brownish-coloured sediment of 1–2 cm thickness and often discontinuous and in one case associated with a calcined bone fragment, we decided to place Trench 1 (excavated in 2017, 2018 and 2022) and Trench 2 (excavated in 2018) close to some of these borings. Trench 2 is positioned 10 m to the northeast of Trench 1 (Fig. 2a and d). Trench 1 covers an area of 5 m by 3 m and is up to 2.3 m deep. Within its sequence, two archaeological horizons (AH) have been documented. Trench 2 has a size of 2 m by 2 m and is up to 2.15 m deep. One AH has been located in the lower part of the Trench 2 sequence.

Methods

Excavation methodology followed standards in Palaeolithic archaeology with piece-plotting all finds > 0.5 cm and wet-sieving all sediments. The methods and digital excavation documentation applied follow those described in Nigst et al., (2014, 2021). After a careful cleaning of the sections, macroscopic descriptions were made by a Quaternary geologist (SP), recording the grain size, the presence and nature of the coarse fraction (> 2 mm), as well as the sedimentary and post-depositional structures including layering, creep, pedality, frost wedges, bioturbations and secondary carbonates (see Haesaerts, 1974; Courty et al., 1989; Bertran, 2004; Goldberg & McPhail, 2006; Pirson & Draily, 2011). We collected samples for soil micromorphology, malacology and biomarkers from the exposed sections.

Laboratory analysis of lithics follows an attribute analysis approach and uses the variables described in Nigst (2012). Faunal analysis includes taphonomic studies using the number of bones (n) as the unit of analysis (Lyman, 2008). The analysis includes breakage types, burning and cortical surface modifications, including human and animal modifications (after Bosch, 2018, Bosch et al., 2024). Animal size classes follow the definitions in Bosch et al. (2024). Charcoal sample cleaning protocol followed the one published by Damblon et al., (1996, see also Damblon & Haesaerts, 2002; Haesaerts, et al., 2010) including identification to at least genus level. For AMS dating, we selected ~ 100 mg of cleaned and identified charcoal. Sample pre-treatment at the Centre for Isotope Research, University of Groningen, employed the ABA procedure (Dee et al., 2020; Mook & Streurman, 1983). AMS dating was conducted at the Centre for Isotope Research using a MICADAS 200 kV accelerator mass spectrometer. The radiocarbon date is presented in radiocarbon years BP with 1σ measurement uncertainty; the calibrated age (calibration curve: IntCal20 [Reimer et al., 2020]; calibration software: OxCal 4.4 [Bronk Ramsey, 2009]) is reported at 95.4% probability.

Lipid extraction was carried out following the methodology described in Jambrina-Enr quez et al. (2024). In summary, the soluble organic content was extracted using ultrasonic extraction with a DCM:MeOH mixture (9:1, v/v). The extract was then separated into different polarity fractions (F1: *n*-alkanes, F2: aromatic hydrocarbons, F3: ketones and *n*-alkyl nitriles, F4: *n*-alkanols and *n*-alkanoic acids) using solid phase extraction and the polar fraction (F4) was derivatized using a silylation procedure. Samples were analysed at the Archaeological Micromorphology and Biomarker Research Laboratory (University of La Laguna, Spain) by gas chromatography with a coupled mass-selective detector (GC-Agilent 7890B, MSD Agilent 5977A) equipped with an HP-5MS capillary column (30 m length × 0.25 mm i.d.,

0.25 μm film thickness) and with helium as the carrier gas (with a flow of 2 mL/min). All measurements were done in duplicate and analysed following the protocol by Jambrina-Enr quez et al. (2024). The compounds were identified by comparing their retention times and mass spectra to the NIST Mass Spectral Database. They were quantified using calibration curves (F1) and by comparing their peak areas to those of known quantities of standards (F2–F4).

For the evaluation of the degradation effect, the odd-over-even predominance (OEP) of the *n*-alkanes patterns (after Zech et al., 2009) and the ratio of long-chain *n*-alkanes to short- and mid-chain *n*-alkanes (LSR) (after Buggle et al., 2010) as well as various long-chain *n*-alkane ratios ($nC31/(nC31 + nC27)$, $nC33/(nC33 + nC27)$ and $nC31/nC31 + nC29$) were utilized (cf. Zech et al., 2012).

Results and Discussion

Excavations in 2017, 2018 and 2022 exposed two sequences in Trench 1 and 2 (Fig. 2d). Both sequences provided small archaeological collections from in total three archaeological horizons.

Trench 1: The sequence of Trench 1 is 2.30 m deep and was extended by coring to 4.25 m (Fig. 3). The sequence is subdivided into 21 stratigraphic units and sub-units (Table 1). Stratigraphic unit (SU) A1 corresponds to relocated humic topsoil while SU A2 is a mix of loessic and humic material due to trench refill by machine, very compacted during relocation of SU A1 by caterpillar. SUs A3-a and A3-b correspond to two horizons of the truncated in situ humic topsoil, Holocene in age.

SU B1 can be interpreted as Pleistocene loessic sediment affected by a biological activity—centimetric greyish beige biogalleries, which are older than the humic topsoil, and older than the migration of secondary carbonates (as they are present as coatings along these biogalleries), so probably Pleistocene in age. This biological activity might be related to a truncated palaeosol. The abundant secondary carbonates, fixed on the biological porosity, are probably related to the Holocene pedogenesis (CCa horizon), and are responsible for the light colour. The wavy lower boundary of SU B1, with tongues oriented downslope, suggests the effect of creep, probably resulting from solifluction. SU C1 is similar to SU B1, but the biological activity is less visible. Again, the wavy lower boundary suggests the effect of solifluction.

SUs B2, C2-b and C4-a are loessic material. SU C2-a probably records a weak tundra gley. SU C3 points to a stabilisation horizon in relation with an archaeological horizon. Possible lateral redistribution of organic matter, charcoal and maybe ash. The upper and lower boundaries of SU C3 are wavy, suggesting an effect of solifluction. Two other possible

Fig. 3 Ollersdorf-Heidenberg, Trench 1: stratigraphic log. Graphic symbols: 1: humic horizon, 2: loess, 3: laminated silt, 4: sandy silt, 5: silty sand, 6: sand, 7: backfill, 8: gravels, 9: molluscs, 10: charcoal, 11: krotovina, 12: small bioturbations, 13: earthworm biogalleries, 14: secondary carbonates (centimetric “loess dolls”), 15: secondary carbonates (pseudomycelium), 16: iron staining, 17: manganese spots, 18: tundra gley, 19: ice wedge pseudomorph, 20: polygonal network of frost wedges, 21: archaeological horizon. Graphic: S. Pirson

small stabilisation surfaces are observed in SU C4-a. The lower half of SU C4, with its laminations (SU C4-b), suggest more humid conditions with reworking of loessic material through run-off.

SUs D1 to D3, with frequent molluscs and small biogalleries, suggest a slower sedimentation rate than overlying SUs. On top of SUs D2 and D3, small dark horizons possibly related to manganese precipitation are observed. SU E1, with iron staining, could indicate hydromorphy; the small exposed part prevents any firm conclusion. SUs E2 to F4 were only observed through the hand auger and, hence, we do not provide interpretations here. They are described as silt, sandy silt, silty sand and sand (for details, see Table 1).

Embedded in this sequence are two AHs (AH Viola and AH Anna). In AH Viola—located in SU C3—we recovered 166 archaeological objects of which 98 were piece-plotted (Table 2). Evidence of human presence is scarce; there are two lithics comprising a proximal flake fragment (Fig. 4: 1; Table 3) and a chip from wet-sieving. All five unidentifiable faunal remains, of which two are calcined, were recovered during wet-sieving and, hence, are < 5 mm (Table 3). Charcoal from SU C3 was identified to *Picea* and *Pinus*, including fragments attributed to *Pinus t. cembra* (Table 4).

AH Anna, located in SU C4-a and about 15 cm below SU C3, is evident from the occurrence of archaeological objects only. We did not observe—on macroscopic scale—any lithostratigraphic change (like the dark/brownish stabilisation horizon with biogalleries in SU C3 with AH Viola). We did note more molluscs at this stratigraphic position relative to above or below within the same stratigraphic unit. AH Anna comprises 71 objects from wet-sieving and 54 objects from piece-plotting (Table 2). Three lithics were piece-plotted comprising a proximal blade fragment (OLL-E19-8) (Fig. 4: 2), a nanogravette point (OLL-C20-10) (Fig. 4: 3) and a core shatter. The nanogravette point suggests a Gravettian attribution of the assemblage. Three faunal remains > 5 mm were piece-plotted and include two rib fragments of ca. 40 cm and ca. 46 cm length (Table 4). No anthropogenic modifications were observed on the faunal remains, but a small portion of the bone fragments retrieved from wet-sieving show traces of burning: 12% ($n=5$) was carbonised and 5% ($n=2$) calcined; the latter suggesting anthropogenic combustion activity (Stiner et al., 1995). Charcoal recovered from AH Anna was identified to *Picea*

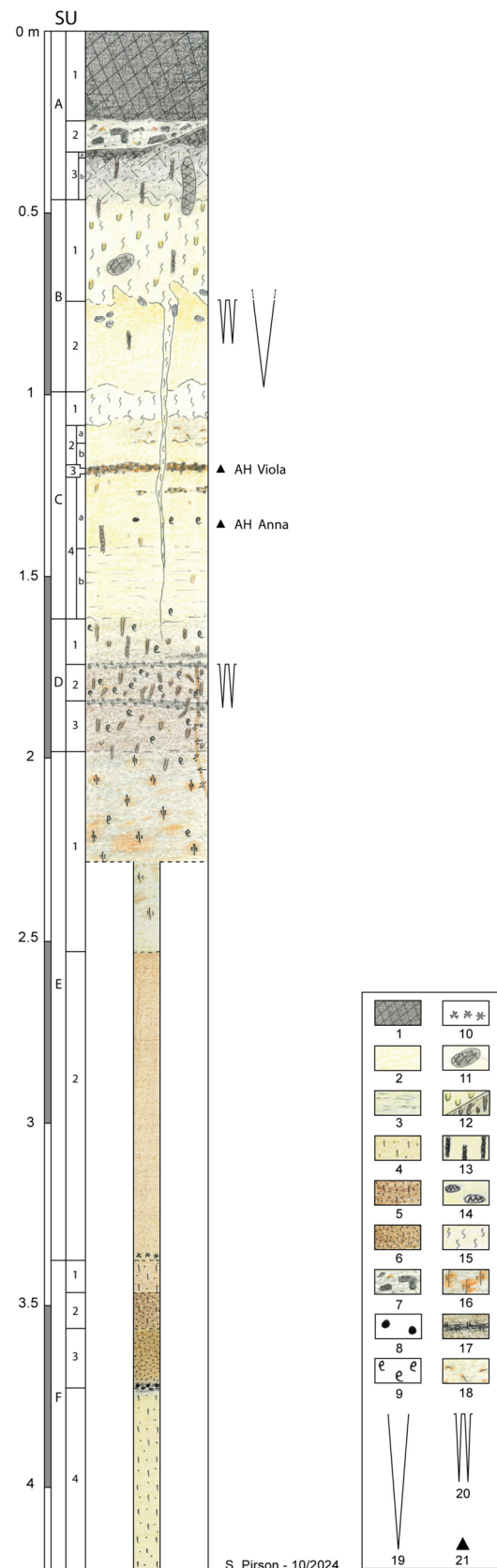


Table 1 Ollersdorf-Heidenberg, Trench 1: List of stratigraphic units recorded including their thickness and lithostratigraphic description. Abbreviations: *SU*, stratigraphic unit; *AH*, archaeological horizon

| SU | Thickness | Lithostratigraphic description |
|-----------------------|-----------|---|
| A1 | 28 cm | Very dark brown to blackish humic silt, rather compact. Locally, towards the bottom of the SU, beige aggregates (mm to pluri-cm) comparable to SU A2. Some reddish ceramic shards (cm). One single cm river pebble (quartz). Granular structure. Bioturbations are frequent: some rodent biogalleries ca. 5 cm (krotovina), numerous earthworms biogalleries, and smaller biogalleries (1–2 mm width). These recent bioturbations, with dark brown to blackish filling, are mainly present in SU A1 to A3-b; they are also locally present throughout the whole profile, although diminishing in number with depth |
| A2 | 10 cm | Very compact beige silt. Numerous mm to pluri-cm aggregates of various colours (most are dark brown, some greyish brown, light greyish beige or beige). Locally, well-expressed platy structure (related to compaction) |
| A3-a | 5 cm | Very dark brown to blackish humic silt. Very compact. Locally absent, this SU can reach up to 13 cm in thickness in squares C21-C22, where lower boundary with SU A3-b is sharp and SU A3-a fills a small depression (=pit?). Granular structure |
| A3-b | 23 cm | Dark brown to greyish brown silt, getting lighter in colour (greyish beige) towards the bottom of the unit (gradual transition with underlying SU B1) |
| B1 | 35 cm | Light greyish beige silt with abundant secondary carbonates. The sediment is rather homogeneous but numerous small bioturbations are present. In addition to recent bioturbations existing throughout the whole profile (see above), presence of small biogalleries with a very homogeneous and compact filling consisting in a greyish beige silt, slightly greenish, appearing darker than the surrounding sediment. These biogalleries are centimetric in width (5–15 mm), globally circular to oval in shape. Secondary carbonates are mainly represented by pseudomycelium throughout the whole SU, but they are also present as centimetric concretions (“loess dolls”) as well as coatings along the greyish beige centimetric biogalleries. In most cases, the lower part of SU B1 is lighter in colour; this is related to enrichment in secondary carbonates. Locally, the upper part of SU B1 is slightly darker in colour. A polygonal network of frost wedges opens at the bottom of SU B1. A probable ice wedge pseudomorph has been observed in the eastern section, opening at the B1/B2 boundary. This boundary is irregular, wavy |
| B2 | 35 cm | Homogeneous beige silt, slightly greyish. Secondary carbonates (mainly pseudomycelium; a few centimetric concretions) are present but in much less abundance than in SU B1. Porosity is much lower than in SU B1 and C1 |
| C1 | 10 cm | Light greyish beige homogeneous silt with abundant secondary carbonates (mainly pseudomycelium; a few centimetric concretions). Some biogalleries (ca. 3 mm in width). Lower boundary is wavy |
| C2 (C2-a and C2-b) | 15 cm | Homogeneous beige silt, slightly more ochre than SU B2. Some secondary carbonates (pseudomycelium and some centimetric concretions). The top of SU C2 is locally more grey (greyish silt) and showed iron staining (SU C2-a). This greyish horizon was only observed in squares C22 and D22 and disappears towards the south (squares C19-21 to E19-21) |
| C3 | 3 cm | Thin dark horizon (5 mm–3 cm thick) characterised by numerous small (3 mm) biogalleries. These biogalleries are most of the time filled with a reddish-brown silt (locally, greyish brown, dark brown or blackish). Both upper and lower boundaries are wavy. SU C3 is more or less continuous on southern and western sections, but is discontinuous to absent on northern and eastern sections. Some recent bioturbations (cf. SU B2). This SU yielded AH Viola |
| C4 (C4-a and C4-b) | 40 cm | Homogeneous beige silt. Locally, in the upper part of SU C4, some 3 to 6 cm below SU C3, a thin and discontinuous horizon similar to SU C3 (although less developed) is present. AH Anna is present ca. 15 cm below SU C3; on the eastern section, a bone fragment and a quartz river pebble can be related to this AH. Rare small (3–4 mm) biogalleries similar to those observed in SU C3 are locally observed throughout the whole SU C4. A few molluscs have been observed in the upper half of the unit. Locally (along the B/C22 section), the lower half of SU C4 shows fine laminations (SU C4-b), while the upper half is homogeneous (SU C4-a). Upper and lower boundaries of SU C4-b are most of the time diffuse and gradual. When the laminations are difficult to distinguish, or absent, distinction between SU C4-a and C4-b is not possible. In some areas, the lower limit of SU C4-b is sharp and erosive on SU D1 |
| D1 | 18 cm | Greyish beige silt, with frequent molluscs. Small (3–4 mm) biogalleries similar to those observed in SU C3 are locally observed throughout the whole sub-unit; they are much more frequent than in SU C4. A few centimetres above the D2/D1 boundary, a small discontinuous darker horizon similar to those on top of SU D2 and D3 is locally present (only on northern section). At the D2/D1 boundary, a polygonal network of frost wedges highlighted by iron hydroxides was observed on several sections and in horizontal view |
| D2 | 10 cm | Greyish beige silt very similar to SU D1, but darker in colour and with more numerous molluscs and more numerous small biogalleries. In the southern part of the western section (square C21 and southern half of C22), a 5- to 30-mm-thick, more or less continuous darker horizon (made of dark millimetric black spots locally coalescing [manganese?]) is present on top of the SU |
| D3 | 18 cm | Greyish beige silt very similar to SU D1, but darker in colour and slightly more greyish. In the southern part of the western section (square C21 and southern half of C22), a 5- to 30-mm-thick, more or less continuous darker horizon was present on top of the sub-unit, similar to that observed on top of SU D2 |

Table 1 (continued)

| SU | Thickness | Lithostratigraphic description |
|----|-----------|--|
| E1 | 58 cm | Grey beige silt with mm to cm sized iron staining. Some molluscs are present throughout the whole sub-unit. The lower half of the unit has only been observed in the coring with the hand auger |
| E2 | 85 cm | Brownish beige silt. This unit, as well as all the underlying units, has only been observed in the coring with the hand auger. Around the transition with underlying SU F1, a few charcoal fragments (2–5 mm) have been observed |
| F1 | 9 cm | Brownish beige sandy silt |
| F2 | 10 cm | Yellowish brown silty sand |
| F3 | 16 cm | Yellowish brown fine to medium sand (more yellow than SU F2). Some carbonate concretions of several millimetres thickness are locally present in the sand |
| F4 | > 50 cm | Yellowish beige sandy silt. The transition with SU F3 is made of light greyish yellow fine sand to silty sand, with small (3–4 mm) river pebbles. Coring with the hand auger was stopped at 1.95 m below the bottom of Trench 1 |

Table 2 Ollersdorf-Heidenberg, Trench 1 and 2: Find numbers per AH

| | | Lithic | Stone | Fauna | Red ochre | Charcoal | Total |
|------------------|---------------|--------|-------|-------|-----------|----------|-------|
| AH Viola, SU C3 | Piece-plotted | 1 | 1 | - | - | 96 | 98 |
| | Wet-sieving | 1 | 18 | 5 | - | 44 | 68 |
| | <i>Total</i> | 2 | 19 | 5 | - | 140 | 166 |
| AH Anna, SU C4-a | Piece-plotted | 3 | 12 | 3 | - | 36 | 54 |
| | Wet-sieving | 1 | 10 | 42 | - | 18 | 71 |
| | <i>Total</i> | 4 | 22 | 45 | - | 54 | 125 |
| AH Steffi, SU Z5 | Piece-plotted | 14 | 13 | 54 | 1 | 123 | 205 |
| | Wet-sieving | 62 | 67 | 610 | 2 | 55 | 796 |
| | <i>Total</i> | 76 | 80 | 664 | 3 | 178 | 1001 |

and *Pinus* (Table 5). A large piece of *Picea* charcoal from sample A-2572 was dated to $24,920 \pm 130$ BP (GrM-19707) (29,535–28,793 cal BP, 95.4% probability). The date corresponds well with the Gravettian attribution based on the presence of a nanogravette point.

Trench 2: The sequence of Trench 2 is 2.15 m deep (Fig. 5) and differs quite substantially from the one of Trench 1 described above. Table 6 presents a detailed description of each lithostratigraphic unit. SU Z1 corresponds to relocated humic topsoil and SU Z2 probably represents two horizons of the truncated in situ humic topsoil, most probably Holocene in age. The underlying SU Z3 (yellowish beige sandy silt with secondary carbonates) can be interpreted as Pleistocene loessic sediment and centrimetric biogalleries are present, resembling those observed in SU B1 in Trench 1. SU Z4 represents the filling of a palaeodepression, which erodes the underlying SU Z5, and is characterised by beige sandy silt to silty sand, with up to several centimetres thick lenses of greenish brown medium to coarse sand. Underlying SU Z5 is a grey beige silt with rust spots and lines (iron staining related to hydromorphy) and secondary carbonates. In the lower portion of the exposed part of SU Z5, about 80 cm below the top of the SU, we observed brownish lenses with abundant charcoal and archaeological objects. These objects were classified as AH Steffi and they form the only

AH in this sequence. AH Steffi amounts to a total of 1001 archaeological objects (205 piece-plotted and 796 collected during wet-sieving). The piece-plotted assemblage is dominated by charcoals, while the material from sieve residues is dominated by faunal fragments (Table 2).

The AH Steffi piece-plotted faunal assemblage—with no species identified due to the fragmented character of the specimens but size classes 2, 3 and 4/5 represented—comprises 54 specimens on which taphonomic investigations were carried out. Cortical surface damage comprises all five weathering stages proposed by Behrensmeyer (1978) with the majority of the remains showing moderate weathering (stage 3) that resulted in cracking of the entire cortical surface without detaching rectangular flakes from its surface (Table 7). Due to the highly fragmentary nature of the assemblage, it was not possible to identify clear primary breakage patterns. Four remains showed rounded edges which would point to abrasion by water and or wind-borne particles, but no smoothing of cortical surfaces was recorded to substantiate this latter hypothesis. No root etching or extensive corrosion of the cortical bone was observed. About 70% of the remains are burned, which contributed substantially to bone fragmentation (see, e.g., Stiner et al., 1995; Clark & Ligouis, 2010). All burning stages after Stiner et al., (1995; see also Reidsma et al., 2016; van Hoesel et al., 2019)

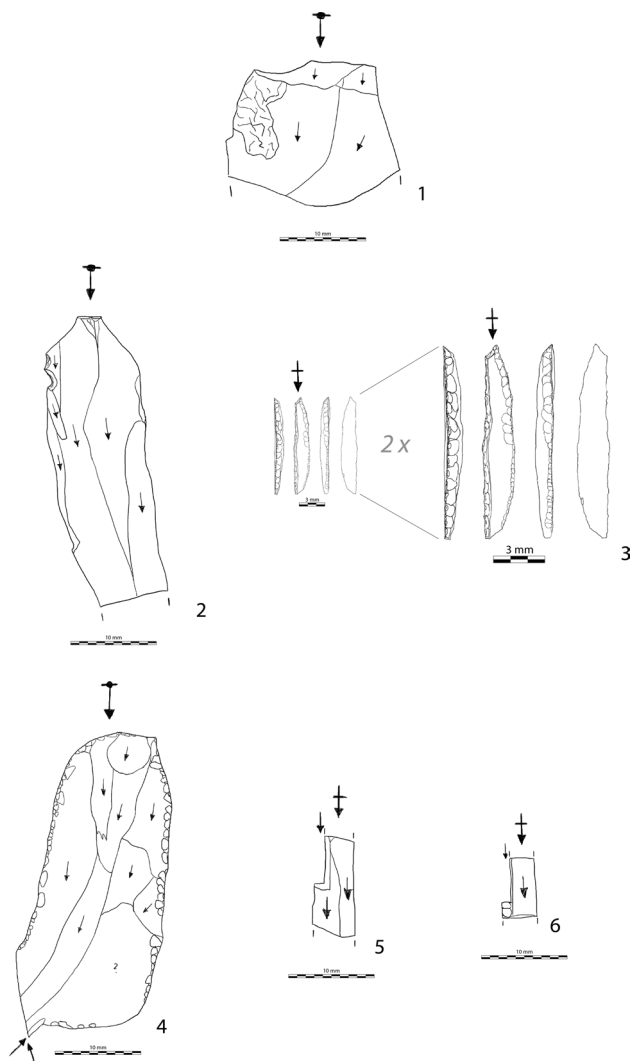


Fig. 4 Ollersdorf-Heidenberg: selected lithic artefacts. 1: Proximal flake fragment with left lateral damage from exposure to heat (OLL-E21-1). 2: Proximal blade fragment (OLL-E19-8). 3: Nanogravette point (OLL-C20-10). 4: Blade with right and left lateral edge retouch and two burin removals on distal end (OLL-B34-1). 5: Medial bladelet fragment with a burin removal on left proximal edge (OLL-B34-85). 6: Medial bladelet fragment with left lateral retouch and burin removal (OLL-B34-3). 1: AH Viola, 2–3: AH Anna, 4–6: AH Steffi. Graphic: P. R. Nigst

were observed with 16% showing various stages of carbonisation while calcination occurs on 53% (Table 8). This suggests anthropogenic combustion activity nearby.

The piece-plotted lithic artefacts ($n = 14$) include four bladelet fragments, two blade fragments, a flake fragment and seven chips. One proximal blade fragment (OLL-B34-1; Fig. 4: 4) is right laterally retouched, one medial bladelet fragment shows a burin removal (OLL-B34-85; Fig. 4: 5) and one medial bladelet fragment (OLL-B34-3; Fig. 4: 6) shows remnants of a lateral retouch, partly removed by a burin blow.

The two sequences of Trench 1 and 2, which are separated by about 10 m distance, show substantial differences in their sequences and we are currently not able to correlate the two sequences (with the exception of the humic top soil). This is probably due to the palaeodepression eroding part of the original Trench 2 sequence. At the moment, it, therefore, has to remain unresolved how AH Steffi of Trench 2 relates to AH Viola and AH Anna in Trench 1.

Preservation of organic matter: Our analysis shows that *n*-alkanes were dominated by long carbon chain lengths with a strong odd/even carbon number preference. All the samples showed a unimodal distribution maximising at *n*C31 (Table 9), which is typical for grassy vegetation and to be expected based on our sequence. If we plot our samples against degradation lines for grassland vs. deciduous trees and shrubs (after Zech et al., 2012), we observe that our samples fall close to the degradation line for grassland (Fig. 6). The *n*-alkane concentration in our samples ranges from 0.32 to 3.24 $\mu\text{g.gds}^{-1}$, while most samples vary between 0.32 and 0.59 $\mu\text{g.gds}^{-1}$ and only sample OLL-SM18-1.1 provided a concentration of 3.24 $\mu\text{g.gds}^{-1}$ (Table 9).

We used the odd-over-even predominance (OEP) of the *n*-alkanes patterns (after Zech et al., 2009) and the ratio of long-chain *n*-alkanes to short- and mid-chain *n*-alkanes (LSR) (after Buggle et al., 2010) as well as various long-chain *n*-alkane ratios ($n\text{C}31/(n\text{C}31 + n\text{C}27)$, $n\text{C}33/(n\text{C}33 + n\text{C}27)$ and $n\text{C}31/n\text{C}31 + n\text{C}29$) to evaluate the degradation effect (cf. Zech et al., 2012). The OEP ranges from 3.91 to 15.23 (Table 9); these values are typical for fresh plant material and modern soils and indicate that plant-derived organic matter at Ollersdorf-Heidenberg is well preserved. Low OEP and LSR correlation (adj. $R^2 = 0.062$; see Fig. 7) indicates that these ratios are more strongly controlled by changes in the alkane patterns of the organic matter and not by post-sedimentary alteration. In sum, the patterns observed indicate good preservation of organic matter.

Comparing our samples from Trench 1 and 2, we do not observe substantial differences (although we need to keep in mind that we have only three samples from Trench 2 while we have 11 samples from Trench 1). OEP, LSR, *n*-alkane concentration and dominant *n*-alkane homologue (C_{max}) do not differ substantially (Table 9). The only sample that stands out in terms of *n*-alkane concentration is sample OLL-SM18-1.1 as mentioned above. We conclude that there is no substantial difference between the two trenches in terms of lipid preservation and in the dominant grassland signal.

The same is true for the three archaeological horizons AH Viola, AH Anna and AH Steffi, despite the fact that AH Viola and AH Steffi are located in brownish sedimentary matrix, while AH Anna occurs in beige silty loess. This might suggest that the different sedimentary matrices are, therefore, not related to differences in vegetation type (i.e. grassland vs. deciduous trees and shrubs).

Table 3 Ollersdorf-Heidenberg: Lithic artefacts (piece-plotted) of AH Anna, AH Viola and AH Steffi

| ID | SU | AH | Category | Raw material | Length | Width | Thickness | Details | Retouch |
|------------|----------|--------|----------------------------|---------------------------|--------|-------|-----------|--|--|
| OLL-C21-16 | C4a | Anna | Core shatter | Coarse-grained chert | 77.55 | – | – | – | – |
| OLL-C20-10 | C4a | Anna | Nanogravette point | Flint, white patinated | 11.28 | 1.98 | 1.1 | – | Nanogravette point |
| OLL-E19-8 | C4a | Anna | Blade proximal fragment | Flint, white patinated | 32.48 | 11.59 | 2.4 | – | Some retouch from use? |
| OLL-E21-1 | C3 | Viola | Flake proximal fragment | Radiolarite, fine grained | 16.76 | 18.59 | 4.01 | Irregular breakage surface (heat exposure) | Some retouch from use? |
| OLL-B34-6 | Z5 brown | Steffi | Chip | Flint, white patinated | <5.00 | – | – | – | – |
| OLL-B35-3 | Z5 brown | Steffi | Chip | Flint, white patinated | 6.02 | 3.19 | 0.59 | – | – |
| OLL-B34-84 | Z5 brown | Steffi | Bladelet proximal fragment | Flint, white patinated | 6.59 | 2.57 | 0.73 | – | – |
| OLL-B34-40 | Z5 brown | Steffi | Bladelet distal fragment | Flint, white patinated | 6.95 | 3.52 | 0.88 | – | – |
| OLL-B34-30 | Z5 brown | Steffi | Chip | Flint, white patinated | <5.00 | – | – | – | – |
| OLL-B34-26 | Z5 brown | Steffi | Chip | Flint, white patinated | <5.00 | – | – | – | – |
| OLL-B34-1 | Z5 brown | Steffi | Blade proximal fragment | Flint, white patinated | 35.69 | 15.77 | 3.38 | – | Right and left lateral edge retouch, distal two burin removals |
| OLL-B34-3 | Z5 brown | Steffi | Bladelet medial fragment | Flint, white patinated | 7.03 | 3.41 | 1.62 | – | Leftlateral retouch scars, rest of retouch removed by burin blow |
| OLL-B34-7 | Z5 brown | Steffi | Chip | Flint, white patinated | <5.00 | – | – | – | – |
| OLL-B34-32 | Z5 brown | Steffi | Chip | Radiolarite, fine grained | <5.00 | – | – | – | – |
| OLL-C34-79 | Z5 brown | Steffi | Chip | Flint, white patinated | 6.37 | 8.47 | 2.43 | – | – |
| OLL-B34-85 | Z5 brown | Steffi | Bladelet medial fragment | Flint, white patinated | 11.26 | 4.4 | 1.55 | – | Leftlateral burin scar |
| OLL-C34-18 | Z5 brown | Steffi | Blade medial fragment | Flint, white patinated | 16.84 | 9.7 | 2.68 | – | – |
| OLL-B34-92 | Z5 brown | Steffi | Flake distal fragment | n/a | 7 | – | – | Exposure to heat (cracks, colour change) | – |

We have three sets of samples that were collected from above, within and below an archaeological horizon. This is the case for the set of OLL-SM18-1.1 (above AH Viola), OLL-SM18-1.2 (AH Viola) and OLL-SM18-1.3 (below AH Viola), the set of OLL-C17-9-1 (above AH Anna), OLL-C17-9-2 (AH Anna) and OLL-C17-9-3 (below AH Anna) and the set of OLL-SM18-2.1 (above AH Steffi), OLL-SM18-2.2 (AH Steffi) and OLL-SM18-2.3 (below AH Steffi). These three sets do not show any substantial

differences in OEP, LSR, *n*-alkane concentration and dominant *n*-alkane homologues below the AH, within the AH and above the AH. This lets us suggest that in terms of lipid preservation and the dominant grassland biomarker signal the AHs are not different from the sediments below and above.

Combustion activity: Calcined and burned faunal remains, abundant charcoals and some lithics exhibiting damage due to exposure to heat have been observed in the

Table 4 Ollersdorf-Heidenberg: Faunal remains (piece-plotted) of AH Anna and AH Steffi. Abbreviations: *NID*, unidentified. Size classes after Bosch et al. (2024)

| ID | SU | AH | Species | Element | Weathering | Burning |
|-------------|----------|--------|----------|--------------------|------------|---------|
| OLL-B34-101 | Z5 brown | Steffi | NID | NID | 1 | 2 |
| OLL-B34-102 | Z5 brown | Steffi | NID | NID | 3 | na |
| OLL-B34-106 | Z5 brown | Steffi | NID | NID | 3 | 2 |
| OLL-B34-19 | Z5 brown | Steffi | NID | NID | na | 0 |
| OLL-B34-2 | Z5 brown | Steffi | NID | NID | 2 | 5 |
| OLL-B34-20 | Z5 brown | Steffi | NID | NID | 3 | 0 |
| OLL-B34-21 | Z5 brown | Steffi | NID | NID | 4 | 6 |
| OLL-B34-22 | Z5 brown | Steffi | NID | NID | na | 0 |
| OLL-B34-23 | Z5 brown | Steffi | NID | NID | na | 6 |
| OLL-B34-24 | Z5 brown | Steffi | SIZE 3 | Long bone fragment | 1 | 4 |
| OLL-B34-25 | Z5 brown | Steffi | NID | NID | 2 | 4 |
| OLL-B34-27 | Z5 brown | Steffi | NID | NID | 3 | 6 |
| OLL-B34-28 | Z5 brown | Steffi | NID | NID | na | 6 |
| OLL-B34-29 | Z5 brown | Steffi | NID | NID | 5 | na |
| OLL-B34-34 | Z5 brown | Steffi | NID | NID | 0 | 3 |
| OLL-B34-35 | Z5 brown | Steffi | SIZE 2 | Sesamoid fragment | 3 | 0 |
| OLL-B34-36 | Z5 brown | Steffi | NID | NID | na | 0 |
| OLL-B34-37 | Z5 brown | Steffi | NID | NID | 3 | na |
| OLL-B34-38 | Z5 brown | Steffi | NID | NID | na | 0 |
| OLL-B34-41 | Z5 brown | Steffi | NID | NID | na | 2 |
| OLL-B34-41a | Z5 brown | Steffi | NID | NID | na | 4 |
| OLL-B34-5 | Z5 brown | Steffi | NID | NID | 4 | 4 |
| OLL-B34-52 | Z5 brown | Steffi | NID | NID | na | 0 |
| OLL-B34-59 | Z5 brown | Steffi | NID | NID | 3 | na |
| OLL-B34-61 | Z5 brown | Steffi | NID | NID | na | 6 |
| OLL-B34-67 | Z5 brown | Steffi | NID | NID | 3 | 4 |
| OLL-B34-68 | Z5 brown | Steffi | NID | NID | 4 | 6 |
| OLL-B34-77 | Z5 brown | Steffi | NID | NID | 4 | 6 |
| OLL-B34-95 | Z5 brown | Steffi | NID | NID | na | 5 |
| OLL-B35-2 | Z5 brown | Steffi | NID | NID | na | 0 |
| OLL-B35-5 | Z5 brown | Steffi | NID | NID | 3 | 5 |
| OLL-C34-10 | Z5 brown | Steffi | NID | NID | na | 0 |
| OLL-C34-15 | Z5 brown | Steffi | NID | NID | 2 | 0 |
| OLL-C34-16 | Z5 brown | Steffi | NID | NID | 3 | 5 |
| OLL-C34-19 | Z5 brown | Steffi | NID | NID | 2 | 5 |
| OLL-C34-2 | Z5 brown | Steffi | NID | NID | na | 0 |
| OLL-C34-22 | Z5 brown | Steffi | NID | NID | na | 6 |
| OLL-C34-28 | Z5 brown | Steffi | NID | NID | na | na |
| OLL-C34-29 | Z5 brown | Steffi | NID | NID | na | 2 |
| OLL-C34-3 | Z5 brown | Steffi | NID | NID | 4 | 0 |
| OLL-C34-30 | Z5 brown | Steffi | NID | NID | na | 5 |
| OLL-C34-32 | Z5 brown | Steffi | NID | NID | na | 5 |
| OLL-C34-35 | Z5 brown | Steffi | SIZE 3 | Long bone fragment | 2 | 5 |
| OLL-C34-40 | Z5 brown | Steffi | SIZE 4–5 | NID | 3 | 1 |
| OLL-C34-41 | Z5 brown | Steffi | NID | NID | 2 | 4 |
| OLL-C34-42 | Z5 brown | Steffi | NID | NID | 3 | 2 |
| OLL-C34-55 | Z5 brown | Steffi | NID | NID | na | 5 |
| OLL-C34-69 | Z5 brown | Steffi | NID | NID | 3 | 0 |
| OLL-C34-7 | Z5 brown | Steffi | NID | NID | na | 0 |
| OLL-C34-8 | Z5 brown | Steffi | NID | NID | na | 6 |
| OLL-C34-80 | Z5 brown | Steffi | NID | NID | 2 | 6 |

Table 4 (continued)

| ID | SU | AH | Species | Element | Weathering | Burning |
|------------|----------|--------|------------------|--------------------|------------|---------|
| OLL-C34-86 | Z5 brown | Steffi | NID | NID | na | 2 |
| OLL-C34-9 | Z5 brown | Steffi | NID | NID | na | 0 |
| OLL-C35-2 | Z5 brown | Steffi | SIZE 2–3 | Long bone fragment | na | 5 |
| OLL-D20-12 | C4-a | Anna | NID | NID | na | 0 |
| OLL-D20-16 | C4-a | Anna | <i>Equus</i> sp. | Rib fragment | 1 | 0 |
| OLL-E19-12 | C4-a | Anna | <i>Equus</i> sp. | Rib fragment | 2 | 0 |

Table 5 Ollersdorf-Heidenberg: Anthracologically analysed charcoal of Trench 1. *RBINS*, Royal Belgian Institute of Natural Sciences; *SU*, stratigraphic unit. *AH*, archaeological horizon

| Laboratory | Excavation IDs of charcoals | SU | AH | Taxon | No charcoal fragments |
|------------|---|--------|----------|---|-----------------------|
| No RBINS | | | | | |
| A-2569 | OLL-C19-27 | SU C3 | AH Viola | <i>Picea</i> | 1 big piece |
| A-2570 | OLL-C19-4 to OLL-C19-20, OLL-C19-22, OLL-C19-23, OLL-C19-29 | SU C3 | AH Viola | <i>Picea</i> <i>Pinus</i> | 45 4 |
| A-2571 | OLL-C20-4, OLL-C20-5, OLL-C20-7 | SU C3 | AH Viola | <i>Pinus t. cembra</i> | 27 |
| A-2566 | OLL-D19-2 to OLL-D19-6 | SU C3 | AH Viola | <i>Picea</i> | 31 |
| A-2567 | OLL-D20-1, OLL-D20-6, OLL-D20-8 to OLL-D20-11, OLL-D20-13, OLL-D20-24, OLL-D20-25 | SU C3 | AH Viola | <i>Picea</i> | 56 |
| A-2572 | OLL-C19-31 to OLL-C19-34, OLL-C19-37 | SU C4a | AH Anna | <i>Picea</i> <i>Pinus</i> cf. <i>Fraxinus</i> | 1 big piece 3 7 |
| A-2568 | OLL-D20-14, OLL-D20-19, OLL-D20-21 | SU C4a | AH Anna | <i>Picea</i> <i>Pinus t. cembra</i> | 3 34 |

archaeological horizons (Table 10), suggesting the presence of some combustion activity during their occupations.

Within Trench 2, the brownish lens in SU Z5—containing the archaeological materials described as AH Steffi—yielded a rich charcoal assemblage as well as calcined faunal remains and one heat-exposed lithic artefact, but we did not observe any macroscopic evidence of potential in situ combustion activity. The same is true for AH Anna (SU C4-a) in Trench 1.

Similarly, AH Viola provided abundant charcoals, two calcined faunal specimens and one heated lithic. In addition, during our 2017 fieldwork in Trench 1, we observed slightly brownish-reddish colouration at the bottom of SU C3 in the 2017 northern section along X-coordinate 1000.30 to 1000.50, in areas also abundant in charcoal. We cannot label this as typically “reddish-heated sediments” (rubification) like the well-documented examples at, e.g., Pavlov I (e.g. Svoboda 2005; Svoboda et al., 2016), Grub-Kranawetberg I (e.g. Antl-Weiser, 2008; Nigst & Antl-Weiser, 2012), Krems-Wachtberg (e.g. Simon et al., 2014) and Korman’ 9 (Kulakovska et al., 2021), all in a loessic context, and at, e.g., Abric del Pastor within a different sedimentary matrix (Mallol et al., 2019). However, in combination with calcined faunal remains and one flake showing damage congruent with heat exposure as well as the presence of abundant charcoals, this

potentially reddened sediment patch warranted a more in-depth testing for the presence of in situ combustion activity by field observations, micromorphology and biomarkers. To test this, we conducted detailed field observations during our 2018 and 2022 fieldwork seasons and collected samples for micromorphological and biomarker analyses.

Our detailed macroscopic field study of the sediments in 2018 and 2022 did not find any evidence of reddish colouration (rubification) in SU C3 or anywhere else in the sequences of both trenches. Micromorphology sample OLL-SM17-3, which was retrieved from the 2017 area in the northern section showing slightly brownish-reddish colouration of SU C3, as well as the samples OLL-SM17-4, OLL-SM17-5 and OLL-SM18-1 covering SU C3/AH Viola does not show any evidence of combustion activity. Also, sample OLL-SM18-2 (SU Z5) in Trench 2 did not provide any microscopic evidence of combustion activity.

Our biomarker analysis did not detect aromatic hydrocarbons, ketones and n-alkyl nitriles in the studied samples OLL-SM17-4.1, OLL-SM17-4.2, OLL-SM18-1.2 (all AH Viola/SU C3), OLL-C17-9–2 (AH Anna/SU C4a) and OLL-SM18-2.2 (AH Steffi/SU Z5 brown), allowing us to exclude in situ combustion activity—whether natural or anthropogenic—as the source of the dark colour of the brownish discontinuous matrix of both SU C3 (AH Viola) and SU

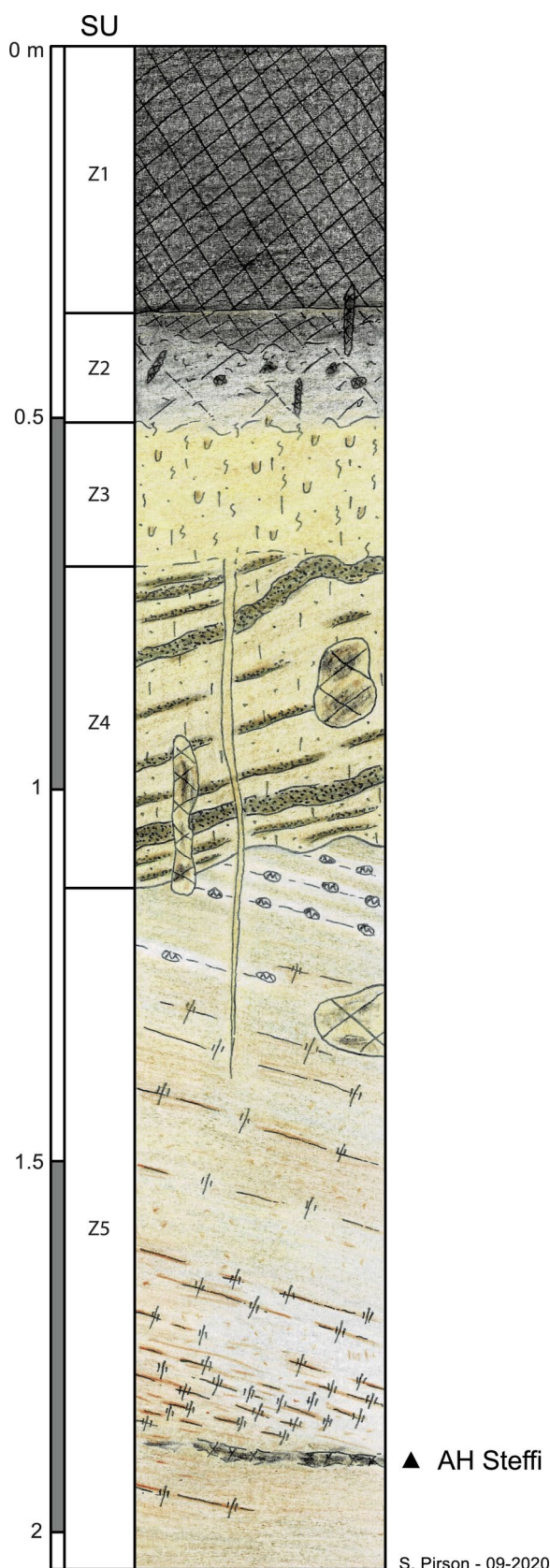


Fig. 5 Ollersdorf-Heidenberg, Trench 2: stratigraphic log. Graphic symbols: see Fig. 3. Graphic: S. Pirson

Z5 (AH Steffi). Also, the samples from SU C4-a (including AH Anna) do not show any evidence of the above markers of in situ combustion activity. This is further supported by the high OEP values observed in all samples.

Taken together, while evidence of direct exposure to fire based on calcined faunal specimens, lithics with typical damage congruent with heat exposure and abundant charcoal fragments, we could observe no evidence of in situ burning using macroscopic, microscopic and molecular approaches. This, in turn, strengthens our above interpretation of SU C3 with AH Viola as potentially representing lateral redistribution of archaeological materials including heated lithics, calcined faunal specimens, organic matter and charcoal from further upslope, which might point to combustion activity there, but no in situ combustion activity within the extent of our excavation trenches.

Comparison of our 2017–2022 results with the 1998 and 2007 fieldwork related to pipeline construction: The lithic artefacts of the 1998 and 2007 fieldwork can be classified as Gravettian and show overall similar features as the 2017–2022 excavation materials; they lack diagnostic tools like backed elements (Antl-Weiser, 2008). However, one should note a nanogravette point collected by a local collector in 1998 from the sediment removed by the caterpillar before the contract archaeology excavations started (Schmitsberger et al., 2018). However, its relationship to the stratified materials reported by Antl-Weiser (2008; see also Antl, 1998, 2007) remains unclear.

An obvious difference between our field record and the 1998 and 2007 field records is that the archaeological horizons of the 1998 and 2007 pipeline trenches are in part associated with brownish layers and—especially in the 2007 trench—also with reddish-coloured sediment (probably from exposure to fire). In some areas of the pipeline trenches, the brown layers are much thicker (up to ~ 12 cm; Antl-Weiser, 2008) than in our fieldwork. The find density in AH Anna and AH Viola seems lower than in the main archaeological horizons of the 1998 and 2007 pipeline trenches. However, over the extent of the pipeline trenches, the find density varies considerably (Antl-Weiser, 2008).

Establishing a potential correlation of our two sequences to the sequences documented in the 1998 and 2007 fieldwork is complicated by the fact that they are separated by at least 10 m. The sequences of the 1998 and 2007 rescue archaeology trenches—although due to the rescue archaeology nature of the operation not studied in as much detail as our sequences—show a somehow similar exposure. Antl-Weiser (2008; Antl, 2007) reports for the 2007 trench two AHs associated with brownish lenses and separated by about 10–15 cm of sterile loessic sediment. About 15–20 cm above the upper AH, a light greyish to beige horizon with abundant secondary carbonates was observed, which could be equivalent to SU C1 in

Table 6 Ollersdorf-Heidenberg, Trench 2: List of stratigraphic units recorded including their thickness and lithostratigraphic description. Abbreviations: *SU*, stratigraphic unit. *AH*, archaeological horizon

| SU | Lithostratigraphic description |
|----|---|
| Z1 | Dark brown to blackish humic silt (backfill) |
| Z2 | Dark brown to greyish beige slightly humic silt. Granular structure. Numerous bioturbations (some rodent biogalleries ca. 5 cm, earthworms biogalleries, and smaller biogalleries 1–2 mm) |
| Z3 | Yellowish beige sandy silt with secondary carbonates. The lower boundary is unclear because of the pedological activity affecting Z3. It is probably erosive (angular discordance). Centrimetric biogalleries similar to those observed in Unit B1 from Trench 1 are present (homogeneous and compact filling of greyish beige silt, slightly greenish, appearing darker than the surrounding sediment); secondary carbonates are also present as coatings along the biogalleries, as in Unit B1 from Trench 1. A wedge opens from the Z4/Z3 boundary |
| Z4 | Beige sandy silt to silty sand, with up to several centimetres thick lenses of greenish brown medium to coarse sand. Erosive lower boundary on Unit Z5. The slope of the sandy lenses suggests the existence of a palaeodepression oriented towards the south-east, with a dip of ca. 10–20° |
| Z5 | Grey beige silt with rust spots and lines (iron staining related to hydromorphy). Secondary carbonates (centrimetric concretions: “loess dolls”), locally aligned. The lines of iron hydroxydes as well as the aligned secondary carbonate are dipping westward (ca. 10°), contrasting with the south-eastern slope of the sandy lenses from Unit Z4. AH Steffi is lying more or less horizontally at the bottom of Trench 2 (lithic artefacts, charcoal and faunal remains) in a brownish discontinuous matrix |

Table 7 Ollersdorf-Heidenberg, Trench 2, AH Steffi: Weathering in the piece-plotted faunal assemblage (excluding spongy bone fragments). Weathering stages after Behrensmeyer (1978)

| Weathering stage | <i>n</i> | % |
|------------------|-----------|--------------|
| 0 | 1 | 3.5 |
| 1 | 2 | 6.9 |
| 2 | 7 | 24.1 |
| 3 | 13 | 44.8 |
| 4 | 5 | 17.2 |
| 5 | 1 | 3.5 |
| Total | 29 | 100.0 |

Table 8 Ollersdorf-Heidenberg, Trench 2, AH Steffi: Burning damage in the piece-plotted faunal assemblage (excluding the decalcified specimens). Burning stages after Stiner et al. (1995)

| Burning stage | <i>n</i> | % |
|---------------|-----------|--------------|
| 0 | 15 | 30.6 |
| 1 | 1 | 2.0 |
| 2 | 6 | 12.3 |
| 3 | 1 | 2.0 |
| 4 | 6 | 12.3 |
| 5 | 10 | 20.4 |
| 6 | 10 | 20.4 |
| Total | 49 | 100.0 |

our Trench 1 sequence (Fig. 8). And, another 30–40 cm higher in the 2007 sequence a light greyish to beige horizon rich in abundant secondary carbonates with occasional deep wedges enriched in secondary carbonates, which could be equivalent to our SU B1 and the network of frost wedges starting from there, was observed. We cannot demonstrate such a correlation but want to highlight here the similarity of the two sequences, keeping in mind that the 2007 sequence has not been studied with the same detail as the 2017, 2018 and 2022 sequences reported here. We should also note a radiocarbon date of 25,450 ± 90 BP (30,006–29,322 cal BP [95.4% probability], VERA-366,

charcoal; Antl-Weiser, 2008) for the lower and richer archaeological horizon in the 1998 pipeline trench, which is slightly older but still overlaps with the calibrated age range (29,535–28,793 cal BP [95.4% probability], see above) of AH Anna charcoal, and, therefore, AH Anna and the lower AH of the 1998 pipeline trench could be contemporaneous. Future fieldwork might be able to establish a correlation if access to the pipeline trench can be organised, which is currently difficult due to security distance of any earthworks to the pipelines.

Chronological position in the regional context: For a discussion of the chronological position of Ollersdorf-Heidenberg 2017–2022 in the regional context of the Middle Danube region, we are limited to the radiocarbon date of AH Anna. We do not have clear chronostratigraphic markers in the Ollersdorf-Heidenberg Trench 1 and 2 sequences to help with correlations. Also, the small lithic assemblages are of limited use for a detailed correlation, as they are lacking chronologically diagnostic markers. The nanogravette point (defined after Maurer [2006]) itself does not represent a chronologically highly sensitive tooltype—it occurs in Early and Late Gravettian contexts both in Central and Western Europe (e.g. Floss et al., 2009; Moreau, 2009, 2012; Taller & Floss, 2011), even if it is sometimes subsumed in microgravette points. Examples are known from Willendorf II, AH 5 and AH 9 (*cf.* drawings in, e.g., Felgenhauer, 1959 and Moreau, 2012)—showing the chronological range of the tooltype—and in Geißenklösterle (Moreau, 2009) and Azé-Camping de Rizerolles (Maurer, 2006; Floss et al., 2009; Taller & Floss, 2011).

Comparing the Trench 1 and 2 sequences of Ollersdorf-Heidenberg with the nearby sequences of Grub-Kranawetberg I (e.g. Antl-Weiser, 2008; Antl-Weiser et al., 2010, 2024a, 2024b) and Grub-Kranawetberg II (Nigst et al., 2024; Bosch et al., in press a, in press b) shows that the

Table 9 Ollersdorf-Heidenberg: Lipid biomarkers and their concentration as detected in the analysed samples (µg/gds). Abbreviations: *OEP* (after Zech et al., 2009), odd-over-even predominance; *LSR* (after Buggle et al., 2010), ratio of long-chain to short-and mid-chain *n*-alkanes; *Cmax*, dominant *n*-alkane homologue; *gds*, gram of dry sediment

| SU/AH | SUC2 bot- tom | SU C3 AH Viola | SU C3 AH Viola | SUC3 AH Viola | SUC4a top | SUC4a brown- ish lenses | SUC4a brown- lenses | SUC4a above Anna | SU C4a above Anna | SU C4a above AH | SU C4a above AH | SU C4a AH Anna | SU C4a below AH | SU Z5 above brownish lenses | SU Z5 above brownish lenses Steffi | SU Z5 below brownish lenses |
|-----------------------|------------------|----------------------|-------------------|------------------|------------------|----------------------------|------------------------|------------------------|-------------------------|-----------------------|-----------------------|-------------------|-----------------------|-----------------------------------|---|--------------------------------------|
| Sample no | OLL- SM18-1.1 | OLL- SM17-4.1 | OLL- SM17-4.2 | OLL- SM18-1.2 | OLL- SM18-1.3 | OLL- SM17-5.1 | OLL- SM17-5.2 | OLL- API7-5 | OLL-C17- 9-1 | OLL-C17- 9-2 | OLL-C17- 9-3 | OLL-C17- 9-3 | OLL- SM18-2.1 | OLL- SM18-2.1 | OLL- SM18-2.2 | OLL- SM18-2.3 |
| Total Alk > 25 µg/gds | 3.24 | 0.45 | 0.41 | 0.49 | 0.40 | 0.32 | 0.38 | 0.34 | 0.49 | 0.51 | 0.59 | 0.57 | 0.56 | 0.51 | 0.56 | 0.51 |
| Cmax | nC31 | nC31 | nC31 | nC31 | nC31 | nC31 | nC31 | nC31 | nC31 | nC31 | nC31 | nC31 | nC31 | nC31 | nC31 | nC31 |
| OEP | 6.26 | 6.39 | 7.19 | 8.21 | 9.11 | 15.23 | 12.17 | 4.13 | 4.18 | 4.02 | 3.91 | 7.51 | 9.89 | 11.92 | 9.89 | 11.92 |
| LSR | 16.28 | 28.69 | 30.98 | 37.57 | 17.75 | 16.68 | 20.98 | 7.07 | 8.50 | 7.17 | 6.00 | 30.30 | 16.79 | 23.21 | 16.79 | 23.21 |
| Monopalmitin µg/gds | - | 0.81 | 2.1 | - | 2.34 | 1.65 | - | 0.48 | - | - | 0.21 | - | - | - | - | - |
| Monoestearin µg/gds | - | - | 1.89 | - | 2.19 | 1.08 | - | 0.24 | - | - | 0.07 | - | - | - | - | - |
| B-Sitosterol µg/gds | - | 0.6 | 0.6 | 5.52 | - | 0.21 | - | - | - | - | - | 3.75 | - | - | - | - |
| Stigmaesterol µg/gds | - | - | - | 0.54 | - | - | - | - | - | - | - | - | - | - | - | - |
| Palmitic acid µg/gds | 13.23 | 4.8 | 19.26 | 3.99 | 14.4 | 5.91 | 2.13 | 2.07 | 1.41 | 1.61 | 1.93 | 4.44 | 22.53 | 12.75 | 22.53 | 12.75 |
| Stearic acid µg/gds | 8.28 | 3.06 | 13.5 | 2.1 | 8.85 | 4.2 | 1.14 | 0.51 | 0.87 | 1.21 | 1.37 | 2.04 | 12.54 | 7.71 | 12.54 | 7.71 |
| Docosanol µg/gds | 1.38 | 0.48 | 0.66 | 1.02 | 0.66 | 0.45 | 0.24 | - | 0.32 | 0.51 | 0.37 | - | 1.17 | 0.57 | 1.17 | 0.57 |
| Tetracosanol µg/gds | 4.08 | 1.02 | 1.8 | 2.82 | 3.12 | 1.23 | 0.69 | 0.09 | 0.67 | 0.71 | 0.07 | 1.02 | 3.78 | 1.98 | 3.78 | 1.98 |
| Hexacosanol µg/gds | 50.34 | 13.11 | 23.43 | 0.42 | 36.57 | 29.13 | 20.01 | 0.21 | 0.29 | 0.25 | 0.29 | 1.08 | 81.45 | 46.38 | 81.45 | 46.38 |
| Octacosanol µg/gds | 27.72 | 3.66 | 7.95 | 14.55 | 15.3 | 4.62 | 3.03 | 0.06 | - | - | - | 17.01 | 37.38 | 24.84 | 37.38 | 24.84 |
| Triacosanol µg/gds | 9.93 | - | 3.12 | 5.13 | 4.47 | 2.07 | 1.35 | - | 0.87 | 0.49 | 0.23 | 8.79 | 17.31 | 14.25 | 17.31 | 14.25 |

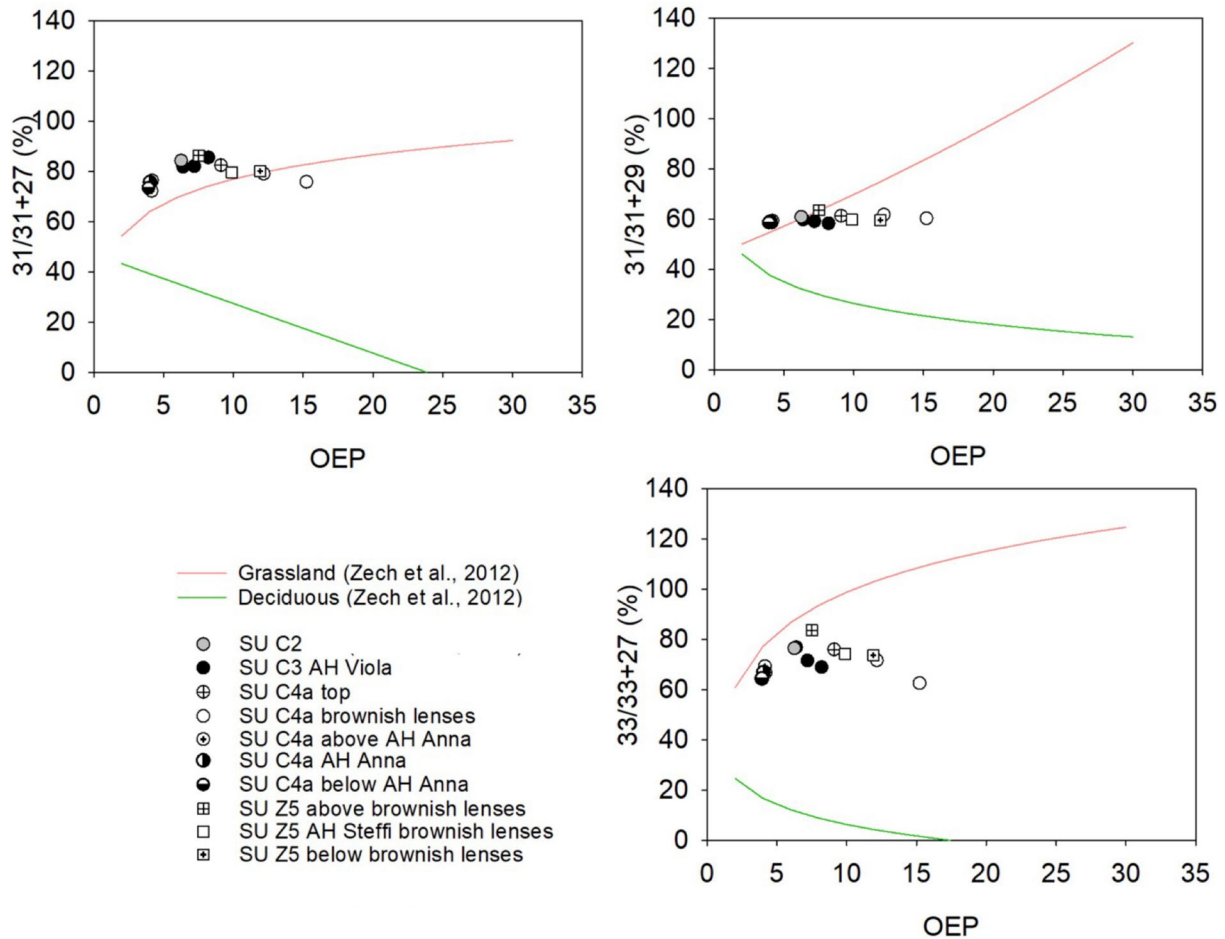


Fig. 6 Ollersdorf-Heidenberg: Analysed biomarker samples plotted against degradation lines (after Zech et al., 2012) for grassland vs. deciduous trees and shrubs. Graphic: M. Jambrina-Enríquez

chronological position of AH Anna at Ollersdorf-Heidenberg (based on the radiocarbon age of 29,535–28,793 cal BP) overlaps with the radiocarbon ages of both AH 4 and AH 3 at Grub-Kranawetberg I (e.g. Antl-Weiser et al., 2010). The AH Anna nanogravette point currently does not have correlates in AH 4 and AH 3 at Grub-Kranawetberg I, but abundant backed pieces including microgravette points have been observed in both AH 4 and AH 3 (Antl, 2013). In the wider region, the radiometric age of AH Anna points towards the beginning of the Late Gravettian in the region and overlaps with the established age range of among others Willendorf II, AH 9 (Austria) (Haesaerts et al., 1996; Nigst et al., 2014), and Trenčianske Bohuslavice, Layer A2-3 (Slovakia) (Wilczyński et al., 2020b).

Concluding Remarks

The data collected during the first research excavations at the open-air site of Ollersdorf-Heidenberg confirm its status as a Mid-Upper Palaeolithic site with three archaeological horizons. The excavations at the site have exposed two sequences in two trenches separated by about 10-m lateral distance. Based on the small lithic collections, we can attribute at least the artefacts of AH Anna to the Gravettian because of the presence of a nanogravette point, which is congruent with the radiocarbon age of associated charcoal. Together, this evidence points to a chronological position at the interface of the Middle to the Late Gravettian. The other two AHs would fit in a Gravettian

Fig. 7 Ollersdorf-Heidenberg: Correlation of OEP and LSR ratios of the analysed lipid biomarker samples in Table 9. Graphic: P. R. Nigst

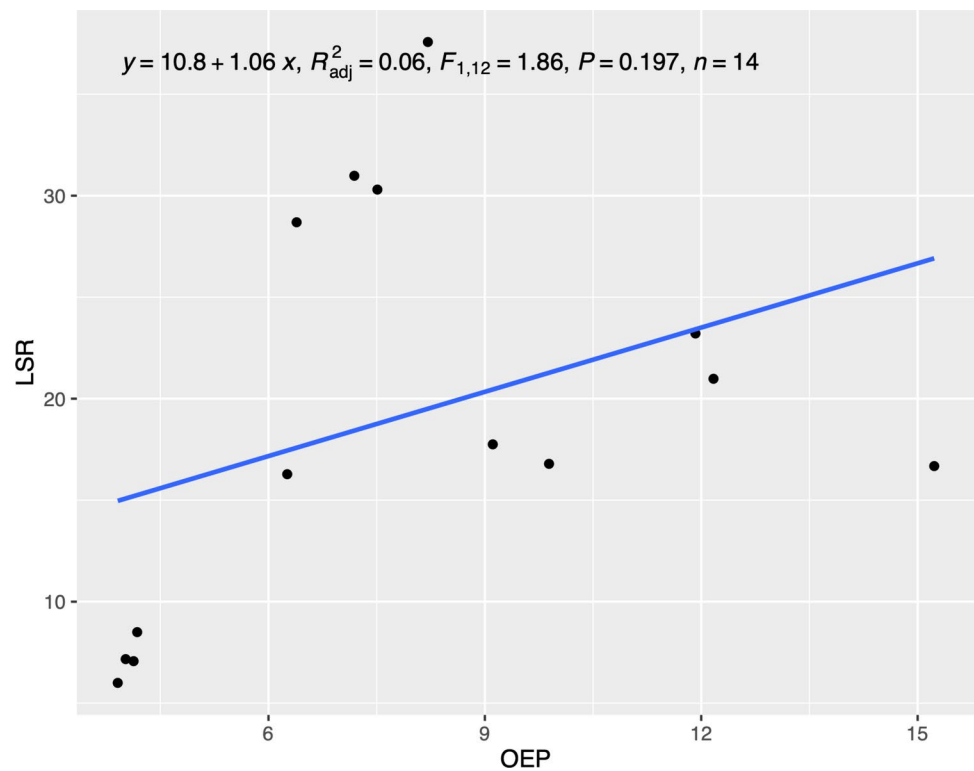


Table 10 Ollersdorf-Heidenberg: Finds showing evidence of fire exposure per AH

| | Lithics with fire damage | Fauna > 5 mm carbonised | Fauna < 5 mm carbonised | Fauna > 5 mm calcined | Fauna < 5 mm calcined | Charcoal |
|-----------|--------------------------|-------------------------|-------------------------|-----------------------|-----------------------|----------|
| | <i>n</i> | <i>n</i> | <i>n</i> | <i>n</i> | <i>n</i> | <i>n</i> |
| AH Viola | 1 | – | 2 | – | 3 | 140 |
| AH Anna | – | – | 2 | – | 5 | 54 |
| AH Steffi | 1 | 8 | 232 | 26 | 142 | 178 |

context; however, they are currently lacking diagnostic lithic features or chronological data. Faunal remains point to size classes 2, 3 and 4/5 but could not be identified to species due to the high fragmentation rate. Faunal collections of all AHs include calcined bone specimens suggesting anthropogenic combustion activity at the site. Macroscopic geological field observations, microscopic geoarchaeological analysis and biomarker analysis suggest no in situ combustion activity in the excavated areas. The two sequences presented show good preservation of charcoal and well-preserved organic matter on molecular level (biomarker analysis).

Given these results, we conclude that Ollersdorf-Heidenberg—despite the low-density area exposed in 2017 to 2022—has good prospects for future field investigations, especially approaches that try to look into organic matter to better understand, e.g. environmental context and plant use. Future work on the materials and samples will focus especially on three themes: palaeoenvironmental and palaeoclimatic context of human occupation, human occupation intensity and combustion activities (and related behaviours) at the site. Reconstructing palaeoenvironmental and palaeoclimatic conditions will include other proxies like molluscs and pollen and apply a multi-scalar (macroscopic

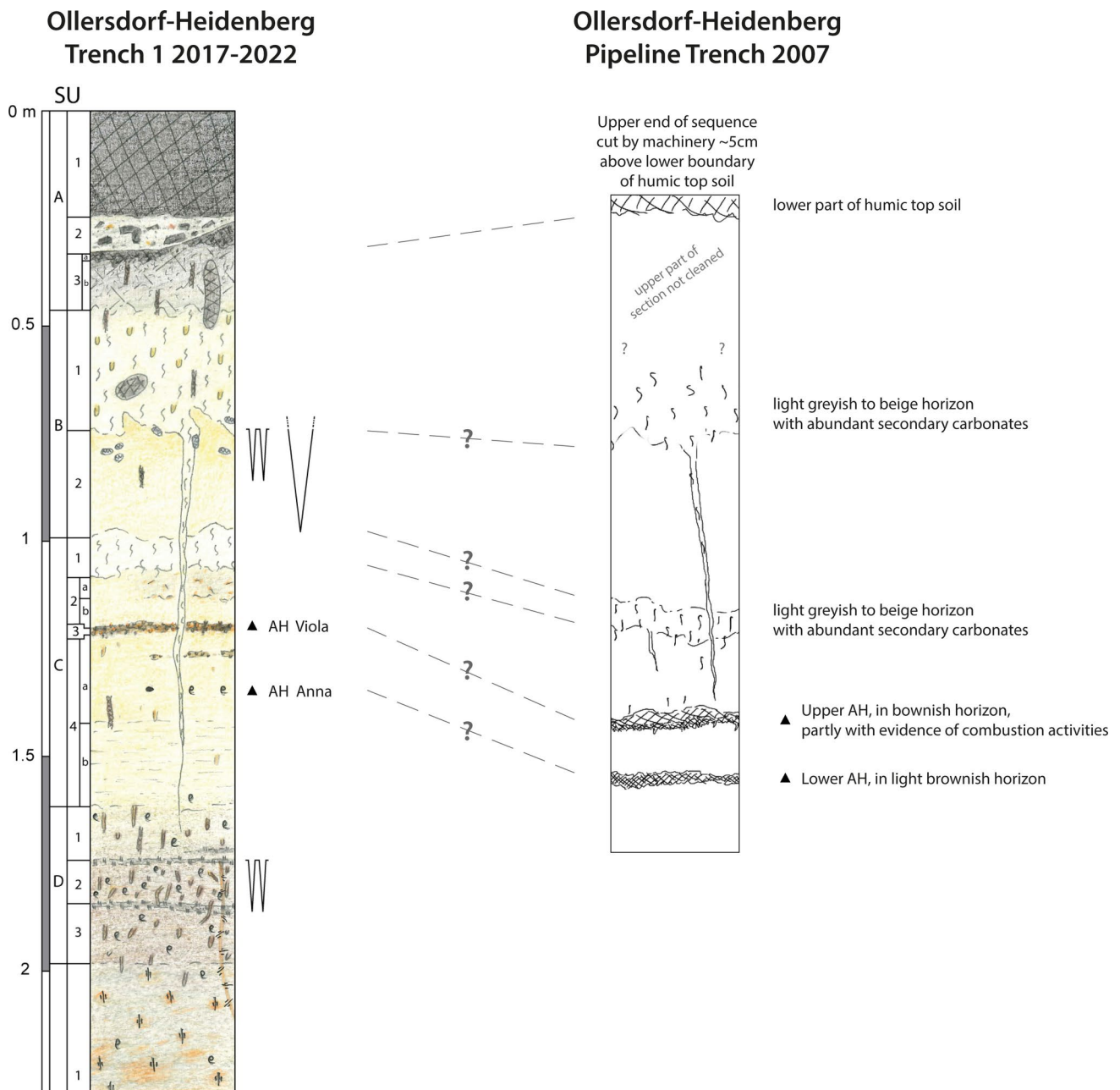


Fig. 8 Potential correlation of the sequences of Ollersdorf-Heidenberg 2017–2022, Trench 1, and Ollersdorf-Heidenberg, Pipeline Trench 2007. Left: Stratigraphic log (S. Pirson) of Ollersdorf-Heidenberg 2017–2022, Trench 1. Graphic symbols: see Fig. 3. Right: Strati-

graphic log constructed from field descriptions and photos provided by W. Antl-Weiser. Both logs are on the same scale. Graphic: P. R. Nigst

– microscopic – molecular) approach, and, thus, provide data to compare to other local (e.g. Grub-Kranawetberg I and II) and regional datasets (e.g. Willendorf sites and Pavlov-Dolní Věstonice sites) and discuss human resilience to climate change at the climatic downturn towards the Last Glacial Maximum. The study of combustion activities including a detailed charcoal analysis and an assessment of potential use of bone as fuel will contribute to larger

questions of fuel and other resource management in a landscape use and settlement dynamics perspective. In a similar vein, the planned investigation of human occupation intensity including geoarchaeological/micromorphological studies will contribute to an approximation of duration of occupation as well as mobility and land use strategies.

In sum, based on the good preservation of organic matter and a multidisciplinary sampling strategy,

Ollersdorf-Heidenberg has a remarkable potential for providing valuable insights in past hunter-gatherer behaviours at the climatic downturn towards the Last Glacial Maximum.

Acknowledgements Many thanks to Andreas Nymark, Hayley Pryor, Viola C. Schmid, Domnika Verdianu, Amanda Darvi, Don Frederik Arthur Maximiliaan van den Biggelaar and the student participants of the 2022 field schools of University of Vienna and University of Toronto for their assistance during fieldwork. We thank Herbert Preisl for permission to use some of his photos of the 2007 pipeline excavation. We thank the landowners (Veith family) for the permission to conduct our fieldwork on their property. Fieldwork has been conducted under the following permits by the Bundesdenkmalamt: 06104.17.01, 06104.17.02 and 06104.18.01 issued to WAW and 06104.22.01 issued to MDB and PRN.

Author Contribution M.D.B. and P.R.N. designed research, M.D.B., P.R.N., S.P. and W.C.M. collected and analysed field data, M.D.B., P.R.N., S.P., F.D., C.M., A.P. and M.J.E. collected and analysed laboratory data, M.D.B., P.R.N., W.A.W. (all 2017–2022) and B.V. (2022) co-directed fieldwork, P.R.N., M.D.B., W.A.W. and B.V. secured fieldwork and analysis funding, W.A.W. contributed contextual data, M.D.B. and P.R.N. wrote first draft of manuscript, all authors contributed and reviewed the final manuscript.

Funding Open access funding provided by University of Vienna. Fieldwork at Ollersdorf-Heidenberg was funded by the DM McDonald Grants and Awards Fund (granting cycle 2017–2018 and 2018–2019), the Department of Prehistory (Natural History Museum, Vienna) (2017 and 2018), the University of Vienna (2022) and the University of Toronto (2022). Fieldwork was further supported by equipment and/or salary funded through an EC FP7 MC Career Integration Grant (grant no. 322261 awarded to PRN, NEMO- ADAP project) and an EC H2020 MSCA Grant (grant no. 656325 awarded to MDB, EU-BEADS project). Travel costs for AP in 2018 were funded by the University of Exeter. The Museumsverein Stillfried-Grub, Austria, supported the fieldwork in 2017 and 2018 through providing accommodation for the team. During the write-up phase of this research MDB has been funded by a Seal-of-Excellence-Fellowship of the Austrian Academy of Sciences, hosted at the Austrian Archaeological Institute, Department of Prehistory and West Asian/Northeast African Archaeology. During preparation of this manuscript PRN was supported by funds from the University of Vienna.

Data Availability Data is either included in the manuscript or is available upon request from the authors.

Declarations

Competing Interests The authors declare no competing interests.

Open Access This article is licensed under a Creative Commons Attribution 4.0 International License, which permits use, sharing, adaptation, distribution and reproduction in any medium or format, as long as you give appropriate credit to the original author(s) and the source, provide a link to the Creative Commons licence, and indicate if changes were made. The images or other third party material in this article are included in the article's Creative Commons licence, unless indicated otherwise in a credit line to the material. If material is not included in the article's Creative Commons licence and your intended use is not permitted by statutory regulation or exceeds the permitted use, you will need to obtain permission directly from the copyright holder. To view a copy of this licence, visit <http://creativecommons.org/licenses/by/4.0/>.

References

- Antl, W. (1998). *KG Ollersdorf. Fundberichte aus Österreich*, 37, 676.
- Antl, W. (2007). *KG Ollersdorf. Fundberichte aus Österreich*, 46, 609–610.
- Antl, W. (2013). The inventories of archaeological horizons 4 and 3 and the loess section of Grub/Kranawetberg, a Gravettian site in Lower Austria. *E&G Quaternary Science Journal*, 62, 120–126.
- Antl-Weiser, W. (2008). Grub/Kranawetberg and Ollersdorf/Heidenberg (Lower Austria) - Two Gravettian camp sites in Eastern Austria. *Wissenschaftliche Mitteilungen Aus Dem Niederösterreichischen Landesmuseum*, 19, 59–78.
- Antl-Weiser, W., Fladerer, F. A., Nigst, P. R., & Verpoorte, A. (2010). Grub/Kranawetberg (Lower Austria) – Insights into a Gravettian Micro-region in Eastern Austria. In C. Neugebauer-Maresch & L. R. Owen (Eds.), *New aspects of the Central and Eastern European Upper Palaeolithic - Methods, chronology, technology and subsistence* (pp. 231–243). Verlag der Österreichischen Akademie der Wissenschaften.
- Antl-Weiser, W., Bosch, D. M., & Nigst, P. R. (2019). Bericht zur Prospektion Ollersdorf-Heidenberg 2017. *Fundberichte aus Österreich*, 56, D2347–D2369.
- Antl-Weiser, W., Bosch, M. D., Pirson, S., & Nigst, P. R. (2024a). Bericht zur Ausgrabung Grub-Kranawetberg 2021. *Fundberichte aus Österreich*, 60, D3514–D3535.
- Antl-Weiser, W., Bosch, M. D., Pirson, S., & Nigst, P. R. (2024b). KG Grub an der March. *Fundberichte aus Österreich*, 60, 246.
- Antl, W., & Bosch, M. D. (2015). The use of ivory at the Gravettian site Grub/Kranawetberg, Lower Austria. *Anthropologie*, LII, 1(1–2), 233–244.
- Bertran, P. (ed.) (2004). *Dépôts de pente continentaux. Dynamique et faciès*. (Quaternaire, hors-série vol. 1). AFEQ, Paris.
- Behrensmeier, A. K. (1978). Taphonomic and ecologic information from bone weathering. *Paleobiology*, 4(2), 150–162.
- Beresford-Jones, D., Taylor, S., Paine, C., Pryor, A., Svoboda, J., & Jones, M. (2011). Rapid climate change in the Upper Palaeolithic: The record of charcoal conifer rings from the Gravettian site of Dolní Věstonice, Czech Republic. *Quaternary Science Reviews*, 30(15–16), 1948–1964. <https://doi.org/10.1016/j.quascirev.2011.04.021>
- Beresford-Jones, D. G., Johnson, K., Pullen, A. G., Pryor, A. J. E., Svoboda, J., & Jones, M. K. (2010). Burning wood or burning bone? A reconsideration of flotation evidence from Upper Palaeolithic (Gravettian) sites in the Moravian Corridor. *Journal of Archaeological Science*, 37(11), 2799–2811. <https://doi.org/10.1016/j.jas.2010.06.014>
- Bosch, D. M. (2018). *Molluscs in the Levantine Upper Palaeolithic: Implications for modern human diets and subsistence behaviour*. Universiteit Leiden, Leiden.
- Bosch, M. D., Kulakovska, L., Usyk, V. I., Kononenko, O., Spry-Marqués, P., & Nigst, P. R. (2024). Human-animal interactions at Korman' 9, Ukraine. *Archaeology and Early History of Ukraine*, 50(1), 119–138. <https://doi.org/10.37445/adiu.2024.01.08>
- Bosch, M. D., Pirson, S., Viola, B. T., Verdianu, D., & Nigst, P. R. (in press a). Bericht zur Ausgrabung Grub-Kranawetberg 2022. *Fundberichte aus Österreich*.
- Bosch, M. D., Pirson, S., Verdianu, D., Kasemann, S., Viola, B. T., & Nigst, P. R. (in press b). Bericht zur Ausgrabung Grub-Kranawetberg 2023. *Fundberichte aus Österreich*.
- Bronk Ramsey, C. (2009). Bayesian analysis of radiocarbon dates. *Radiocarbon*, 51(1), 337–360.
- Buggle, B., Wiesenberger, G. L., & Glaser, B. (2010). Is there a possibility to correct fossil n-alkane data for postsedimentary alteration effects? *Applied Geochemistry*, 25(7), 947–957.

- Cichocki, O., Knibbe, B., & Tillich, I. (2014). Archaeological significance of the Palaeolithic charcoal assemblage from Krems-Wachtberg. *Quaternary International*, 351, 163–171. <https://doi.org/10.1016/j.quaint.2013.07.004>
- Clark, J. L., & Ligouis, B. (2010). Burned bone in the Howieson's Poort and post-Howieson's Poort Middle Stone Age deposits at Sibudu (South Africa): Behavioral and taphonomic implications. *Journal of Archaeological Science*, 37(10), 2650–2661. <https://doi.org/10.1016/j.jas.2010.06.001>
- Courty, M.-A., Goldberg, P., & Macphail, R. I. (1989). *Soils and micro-morphology in archaeology*. Cambridge University Press.
- Damblon, F., & Haesaerts, P. (2002). Anthracology and radiochronology of the Upper Pleistocene in the loessic areas of Eurasia. In S. Thiébauld (Ed.), *Charcoal Analysis. Methodological Approaches, Palaeoecological Results and Wood Uses*. Archaeopress, Oxford, 65–71.
- Damblon, F., Haesaerts, P., & van der Plicht, J. (1996). New datings and considerations on the chronology of Upper Palaeolithic sites in the Great Eurasian Plain. *Préhistoire Européenne*, 9, 177–231.
- Dee, M. W., Palstra, S. W. L., Aerts-Bijma, A. T., Bleeker, M. O., de Bruijn, S., Ghebru, F., Jansen, H., Kuitens, M., Paul, D., Richie, R. R., Spruiensma, J. J., Scifo, A., van Zonneveld, D., Verstappen-Dumoulin, B., Wietzes-Land, P., & Meijer, H. A. J. (2020). Radiocarbon dating at Groningen: New and updated chemical pretreatment procedures. *Radiocarbon*, 62(1), 63–74. <https://doi.org/10.1017/rdc.2019.140>
- Einwögerer, T. (2000). *Die jungpaläolithische Station auf dem Wachtberg in Krems, NÖ: Eine Rekonstruktion und wissenschaftliche Darlegung der Grabung von J. Bayer aus dem Jahre 1930*. Mitteilungen der Prähistorischen Kommission. Verlag der Österreichischen Akademie der Wissenschaften, Vienna.
- Felgenhauer, F. (1959). *Willendorf in der Wachau. Monographie der Paläolith-Fundstellen I-VII* (Mitteilungen der Prähistorischen Kommission VIII+IX). Rohrer, Vienna.
- Felgenhauer, F. (1980). Ein jungpaläolithisches Steinschlägeratelier aus Stillfried an der March, Niederösterreich: Zur Herstellungstechnik von Microgravettespitzen. *Forschungen in Stillfried*, 4, 7–41.
- Floss, H., Dutkiewicz, E., Frick, J., & Hoyer, C. (2009). Le Paléolithique supérieur ancien en Bourgogne du sud. In P. Bodu, L. Chehmana, L. Klaric, L. Mevel, S. Soriano, & N. Teyssandier (Eds.), *Le Paléolithique supérieur ancien de l'Europe du Nord-Ouest: réflexions et synthèses à partir d'un projet collectif de recherche sur le centre et le sud du Bassin parisien* (pp. 331–350). Société préhistorique française.
- Gamble, C. (1999). *The Palaeolithic Societies of Europe*. Cambridge University Press.
- Goldberg, P., & Macphail, R. I. (2006). *Practical and theoretical geo-archaeology*. Blackwell Publishing.
- Haesaerts, P. (1974). Séquence paléoclimatique du Pléistocène supérieur du bassin de la Haine (Belgique). *Annales de la Société Géologique de Belgique*, 97(1), 105–137.
- Haesaerts, P., Damblon, F., Bachner, M., & Trnka, G. (1996). Revised stratigraphy and chronology of the Willendorf II sequence, Lower Austria. *Archaeologia Austriaca*, 80, 25–42.
- Haesaerts, P., Borziac, I., Chekha, V. P., Chirica, V., Damblon, F., Drozdov, N. I., Orlova, L. A., Pirson, S., & van der Plicht, J. (2009). Climatic signature and radiocarbon chronology of Middle and Late Pleniglacial loess from Eurasia: Comparison with the marine and Greenland records. *Radiocarbon*, 51(1), 301–318.
- Haesaerts, P., Borziac, I., Chekha, V. P., Chirica, V., Drozdov, N. I., Koulakovska, L., Orlova, L. A., van der Plicht, J., & Damblon, F. (2010). Charcoal and wood remains for radiocarbon dating Upper Pleistocene loess sequences in Eastern Europe and Central Siberia. *Palaeogeography, Palaeoclimatology, Palaeoecology*, 291(1–2), 106–127.
- Haesaerts, P., Damblon, F., Gerasimenko, N., Spagna, P., & Pirson, S. (2016). The Late Pleistocene loess-palaeosol sequence of Middle Belgium. *Quaternary International*, 411, 25–43. <https://doi.org/10.1016/j.quaint.2016.02.012>
- Hromada, J., & Kozłowski, J. K. (1995). *Complex of Upper Palaeolithic sites near Moravany, Western Slovakia, Vol. 1, Moravany-Žakovska (excavations 1991–1992)*. Institute of Archaeology - Jagellonian University, Krakow.
- Jambrina-Enríquez, M., Mallol, C., Herrera Herrera, A. V., Gonzalez-Urquijo, J., & Lazuen, T. (2024). Microstratigraphic, lipid biomarker and stable isotope study of a middle Palaeolithic combustion feature from Axlor, Spain. *iScience*, 27(1), 108755. <https://doi.org/10.1016/j.isci.2023.108755>
- Kozłowski, J. K. (Ed.). (1998). *Complex of Upper Palaeolithic sites near Moravany, Western Slovakia, Vol. 2, Moravany-Lopata II (excavations 1993 - 1996)*. Institute of Archaeology - Jagellonian University, Krakow.
- Kulakovska, L., Kononenko, O., Haesaerts, P., Pirson, S., Spry-Marqués, P., Bosch, M. D., Popova, L., Popiuk, Y., Damblon, F., Usik, V., & Nigst, P. R. (2021). The new Upper Palaeolithic site Korman' 9 in the Middle Dniester valley (Ukraine): Human occupation during the Last Glacial Maximum. *Quaternary International*, 587–588, 230–250. <https://doi.org/10.1016/j.quaint.2021.02.021>
- Lengyel, G., & Wilczyński, J. (2018). The Gravettian and the Epigravettian chronology in eastern central Europe: A comment on Böskén et al. (2017). *Palaeogeography, Palaeoclimatology, Palaeoecology*, 506, 265–269. <https://doi.org/10.1016/j.palaeo.2017.11.017>
- Mallol, C., Hernández, C., Mercier, N., Falguères, C., Carrancho, Á., Cabanes, D., Vidal-Matutano, P., Connolly, R., Pérez, L., Mayor, A., Ben Arous, E., & Galván, B. (2019). Fire and brief human occupations in Iberia during MIS 4: Evidence from Abric del Pastor (Alcoy, Spain). *Scientific Reports*, 9(1). <https://doi.org/10.1038/s41598-019-54305-9>
- Mason, S. L. R., Hather, J. G., & Hillman, G. C. (1994). Preliminary investigation of the plant macro-remains from Dolní Věstonice II, and its implications for the role of plant foods in Palaeolithic and Mesolithic Europe. *Antiquity*, 68, 48–57.
- Maurer, U. (2006). *Die Silexwerkzeuge der gravettienzeitlichen Freilandfundstelle Azé-Camping de Rizerolles (Saône-et-Loire, Frankreich)*. Master dissertation University of Tübingen.
- Mook, W. G., & Streurman, H. J. (1983). *Physical and chemical aspects of radiocarbon dating*. Proceedings from PACT, Council of Europe.
- Moreau, L. (2009). *Geißenklosterle. Das Gravettien der Schwäbischen Alb im europäischen Kontext*. Kerns Verlag.
- Moreau, L. (2012). Le Gravettien ancien d'Europe centrale revisité : Mise au point et perspectives. *L'anthropologie*, 116(5), 609–638. <https://doi.org/10.1016/j.anthro.2011.10.002>
- Moreau, L., Draily, C., Cordy, J.-M., Boyle, K., Buckley, M., Gjesfjeld, E., Filzmoser, P., Borgia, V., Gibson, S. A., Day, J., Beyer, R., Manica, A., Vander Linden, M., de Grooth, M., & Pirson, S. (2021). Adaptive trade-offs towards the last glacial maximum in North-Western Europe: A multidisciplinary view from Walou Cave. *Journal of Paleolithic Archaeology*, 4(2), 4. <https://doi.org/10.1007/s41982-021-00078-5>
- Neugebauer-Maresch, C. (2008). *Krems-Hundssteig – Mammutjägerlager der Eiszeit. Ein Nutzungsareal paläolithischer Jäger- und Sammler(innen) vor 41.000–27.000 Jahren* (Mitteilungen der Prähistorischen Kommission 67). Verlag der Österreichischen Akademie der Wissenschaften, Vienna.
- Nigst, P. R. (2012). *The Early Upper Palaeolithic of the Middle Danube Region*. Leiden University Press.
- Nigst, P. R., & Antl-Weiser, W. (2012). Les structures d'occupation gravettiennes en Europe centrale: Le cas de Grub/Kranawetberg,

- Autriche. *L'anthropologie*, 116(5), 639–664. <https://doi.org/10.1016/j.anthro.2012.09.001>
- Nigst, P. R., Haesaerts, P., Damblon, F., Frank-Fellner, C., Mallol, C., Viola, B., Göttinger, M., Niven, L., Trnka, G., & Hublin, J.-J. (2014). Early modern human settlement of Europe north of the Alps occurred 43,500 years ago in a cold steppe-type environment. *Proceedings of the National Academy of Sciences*, 111(40), 14394–14399. <https://doi.org/10.1073/pnas.1412201111>
- Nigst, P. R., Libois, T., Haesaerts, P., Bosch, M. D., Branscombe, T., Chirica, V., & Noiret, P. (2021). The Mid Upper Palaeolithic (Gravettian) sequence of Mitoc-Malu Galben (Romania): New fieldwork between 2013 and 2016 - Preliminary results and perspectives. *Quaternary International*, 587–588, 189–209. <https://doi.org/10.1016/j.quaint.2020.10.046>
- Nigst, P. R., Antl-Weiser, W., & Bosch, M. D. (2024). Exploring the surrounding of a Gravettian site. The case study Grub-Kranawetberg. *Austria. Archaeologia Austriaca*, 108, 201–224. <https://doi.org/10.1553/archaeologia108s201>
- Oliva, M. (1988). A Gravettian site with mammoth-bone dwelling in Milovice (Southern Moravia). *Anthropologie*, XXV, 1(2), 105–112.
- Oliva, M. (2009). *Milovice: Site of the Mammoth people below the Pavlov Hills. The question of Mammoth bone structures*. Moravské zemské museum, Brno.
- Pirson, S. & Draily, C. (2011). Lithostratigraphie et genèse des dépôts de la grotte Walou. In: Pirson, S., Draily, C. & Toussein, M. (eds.), *La grotte Walou à Trooz (Belgique). Feuilles de 1996 à 2004. Volume 1. Les sciences de la terre*. (Etudes et documents – Archéologie vol. 20). Service public de Wallonie, Namur, 72–131.
- Polanská, M., & Hromadová, B. (2015). Réflexion autour des industries gravettiennes «post-pavloviennes» de Slovaquie occidentale et de Moravie (25,500/24,500–22,000 BP non calibré). In Sazelova, S., Novak, M., & Mizerova, A. (Eds.), *Forgotten times and spaces: New perspectives in paleoanthropological, paleoetiological and archeological studies*. Institute of Archeology of the Czech Academy of Sciences, Brno, 132–154.
- Pryor, A. J. E., Steele, M., Jones, M. K., Svoboda, J., & Beresford-Jones, D. G. (2013). Plant foods in the Upper Palaeolithic at Dolní Věstonice? Parenchyma redux. *Antiquity*, 87(338), 971–984.
- Rasmussen, S. O., Bigler, M., Blockley, S. P., Blunier, T., Buchardt, S. L., Clausen, H. B., Cvijanovic, I., Dahl-Jensen, D., Johnsen, S. J., Fischer, H., Gkinis, V., Guillevic, M., Hoek, W. Z., Lowe, J. J., Pedro, J. B., Popp, T., Seierstad, I. K., Steffensen, J. P., Svensson, A. M., ... Winstrup, M. (2014). A stratigraphic framework for abrupt climatic changes during the Last Glacial period based on three synchronized Greenland ice-core records: Refining and extending the INTIMATE event stratigraphy. *Quaternary Science Reviews*, 106, 14–28. <https://doi.org/10.1016/j.quascirev.2014.09.007>
- Reidsma, F. H., van Hoesel, A., van Os, B. J. H., Megens, L., & Braadbaart, F. (2016). Charred bone: Physical and chemical changes during laboratory simulated heating under reducing conditions and its relevance for the study of fire use in archaeology. *Journal of Archaeological Science: Reports*, 10, 282–292. <https://doi.org/10.1016/j.jasrep.2016.10.001>
- Reimer, P. J., Austin, W. E. N., Bard, E., Bayliss, A., Blackwell, P. G., Bronk Ramsey, C., Butzin, M., Cheng, H., Edwards, R., Friedrich, M., Grootes, P., Guilderson, T., Hajdas, I., Heaton, T., Hogg, A., Hughen, K., Kromer, B., Manning, S., Muscheler, R., ... Talamo, S. (2020). The IntCal20 Northern Hemisphere radiocarbon age calibration curve (0–55 cal kBP). *Radiocarbon*, 62(4), 725–757. <https://doi.org/10.1017/rdc.2020.41>
- Revedin, A., Aranguren, B., Becattini, R., Longo, L., Marconi, E., Lippi, M. M., Skakun, N., Sinitsyn, A., Spiridonova, E., & Svoboda, J. (2010). Thirty thousand-year-old evidence of plant food processing. *Proceedings of the National Academy of Sciences*, 107(44), 18815–18819. <https://doi.org/10.1073/pnas.1006993107>
- Schilt, F., Verpoorte, A., & Antl, W. (2017). Micromorphology of an Upper Paleolithic cultural layer at Grub-Kranawetberg, Austria. *Journal of Archaeological Science: Reports*, 14, 152–162. <https://doi.org/10.1016/j.jasrep.2017.05.041>
- Schmitsberger, O., Brandl, M., & Trnka, G. (2018). Typical Gravette retouching on “Nano Gravette points” – Meaningful form or formal constraint? Considerations from the study of a Nano Gravette point from Northern Lower Austria in a private collection. In C. M. Lazarovici & A. Berzovan (Eds.), *Quaestiones Praehistoricae. Studia in honorem Professoris Vasile Chirica*. Editura Academiei Române - Editura Istros, Bucurest and Brăila, 75–86.
- Simon, U., Händel, M., Einwögerer, T., & Neugebauer-Maresch, C. (2014). The archaeological record of the Gravettian open air site Krems-Wachtberg. *Quaternary International*, 351, 5–13.
- Skrdla, P. (2005). *The Upper Paleolithic on the Middle Course of the Morava River* (The Dolní Vestonice Studies 13). Academy of Sciences of the Czech Republic.
- Stiner, M. C., Kuhn, S. L., Weiner, S., & Bar-Yosef, O. (1995). Differential burning, recrystallization, and fragmentation of archaeological bone. *Journal of Archaeological Science*, 22(2), 223–237. <https://doi.org/10.1006/jasc.1995.0024>
- Svoboda, J. (Ed.). (2005). *Pavlov I - Southeast. A Window into the Gravettian Lifestyles* (The Dolní Vestonice Studies Vol. 14). Institute of Archaeology, Brno.
- Svoboda, J. A. (2015). Perspectives on the Upper Palaeolithic in Eurasia: The case of the Dolní Vestonice-Pavlov Sites. In N. Sanz (Ed.), *Human origin sites and the World Heritage Convention in Eurasia*. United Nations Educational, Scientific and Cultural Organization, Ciudad de Mexico, 190–204.
- Svoboda, J. (2016). Settlement units and human fossils. Spatial context, stratigraphies and chronology. In J. Svoboda (Ed.), *Chronostratigraphy, Paleoethnology, Paleoanthropology, Dolní Věstonice II*, The Dolní Vestonice Studies (pp. 16–48). Academy of Sciences of the Czech Republic, Institute of Archaeology.
- Svoboda, J. A., Ložek, V., Svobodova, H., & Škrdla, P. (1994). Předmostí after 110 years. *Journal of Field Archaeology*, 21(4), 457–472.
- Svoboda, J. A., Ložek, V., & Vlček, E. (1996). *Hunters between East and West*. Plenum Press, New York.
- Svoboda, J. A., Klíma, B., Jarosová, L., & Škrdla, P. (1999). The Gravettian in Moravia: Climate, behaviour and technological complexity. In W. Roebroeks, M. Mussi, J. Svoboda, & K. Fennema (Eds.), *Hunters of the Golden Age: The Mid Upper Palaeolithic of Eurasia 30000–20000 BP* (pp. 197–217). University of Leiden.
- Svoboda, J. A., Bocheňski, Z. M., Čulíková, V., Dohnalová, A., Hladilová, S., Hložek, M., Horáček, I., Ivanov, M., Králík, M., Novák, M., Pryor, A. J. E., Sázlová, S., Stevens, R., Wilczyński, J., & Wojtal, P. (2011). Paleolithic hunting in a southern Moravian landscape: The case of Milovice IV. *Czech Republic. Geoarchaeology*, 26(6), 838–866. <https://doi.org/10.1002/gea.20375>
- Svoboda, J., Hladilová, Š., Horáček, I., Kaiser, J., Králík, M., Novák, J., Novák, M., Pokorný, P., Sázlová, S., Smolíková, L., & Zikmund, T. (2015). Dolní Věstonice IIa: Gravettian microstratigraphy, environment, and the origin of baked clay production in Moravia. *Quaternary International*, 359–360, 195–210. <https://doi.org/10.1016/j.quaint.2014.06.048>
- Svoboda, J., Krejčí, O., Krejčí, V., Dohnalová, A., Sázlová, S., Wilczyński, J., & Wojtal, P. (2019). Pleistocene landslides and mammoth bone deposits: The case of Dolní Věstonice II. *Czech Republic. Geoarchaeology*, 34(6), 745–758. <https://doi.org/10.1002/gea.21740>

- Svoboda, J., Novák, M., Sázelová, S., & Demek, J. (2016). Pavlov I: A large Gravettian site in space and time. *Quaternary International*, 406, 95–105. <https://doi.org/10.1016/j.quaint.2015.09.015>
- Taller, A., & Floss, H. (2011). Die lithische Technologie der Gravettien-Fundstelle Azé-Camping de Rizerolles (Dép. Saône-et-Loire): Der Fundplatz und seine Forschungsgeschichte. *Archäologisches Korrespondenzblatt*, 41(2), 155–171.
- van Hoesel, A., Reidsma, F. H., van Os, B. J. H., Megens, L., & Braadbaart, F. (2019). Combusted bone: Physical and chemical changes of bone during laboratory simulated heating under oxidising conditions and their relevance for the study of ancient fire use. *Journal of Archaeological Science: Reports*, 28, 102033. <https://doi.org/10.1016/j.jasrep.2019.102033>
- Verpoorte, A. (2001). *Places of art, traces of fire: A contextual approach to anthropomorphic figurines in the Pavlovian (Central Europe, 29-24 kyr BP)*. (ASLU8). Leiden University.
- Verpoorte, A. (2004). Eastern Central Europe during the Pleniglacial. *Antiquity*, 78(300), 257–266. <https://doi.org/10.1017/S0003598X0011292X>
- Wilczyński, J. (2016). Variability of Late Gravettian lithic industries in southern Poland: A case study of the Kraków Spadzista and Jaksice II sites. *Quaternary International*, 406, 129–143. <https://doi.org/10.1016/j.quaint.2015.10.026>
- Wilczyński, J., Goslar, T., Wojtal, P., Oliva, M., Göhlich, U. B., Antl-Weiser, W., Šída, P., Verpoorte, A., & Lengyel, G. (2020a). New radiocarbon dates for the Late Gravettian in Eastern Central Europe. *Radiocarbon*, 62(1), 243–259. <https://doi.org/10.1017/rdc.2019.111>
- Wilczyński, J., Žaár, O., Nemergut, A., Kufel-Diakowska, B., Hoyo, M.M.-D., Mroczek, P., & Lengyel, G. (2020b). The Upper Palaeolithic at Trenčianske Bohuslavice, Western Carpathians. *Slovakia. Journal of Field Archaeology*, 45(4), 270–292. <https://doi.org/10.1080/00934690.2020.1733334>
- Wojtal, P., Wilczyński, J., & Haynes, G. (Eds.). (2015). *Kraków Spadzista: A Gravettian site in Southern Poland*. ISEA PAS.
- Zech, M., Buggle, B., Leiber, K., Marković, S., Glaser, B., Hambach, U., Huwe, B., Stevens, T., Sümegei, P., Wiesenberger, G., & Zöller, L. (2009). Reconstructing Quaternary vegetation history in the Carpathian Basin, SE-Europe, using n-alkane biomarkers as molecular fossils: Problems and possible solutions, potential and limitations. *E&G Quaternary Science Journal*, 58(2), 148–155. <https://doi.org/10.3285/eg.58.2.03>
- Zech, M., Rass, S., Buggle, B., Löscher, M., & Zöller, L. (2012). Reconstruction of the late Quaternary paleoenvironments of the Nussloch loess paleosol sequence, Germany, using n-alkane biomarkers. *Quaternary Research*, 78(2), 226–235.

Publisher's Note Springer Nature remains neutral with regard to jurisdictional claims in published maps and institutional affiliations.

Authors and Affiliations

Marjolein D. Bosch^{1,2,3}  · Stéphane Pirson^{4,5}  · Freddy Damblon⁶ · Margarita Jambrina-Enríquez^{7,8}  · Carolina Mallol^{7,9}  · Alexander Pryor¹⁰ · William Chase Murphree¹¹  · Bence T. Viola¹²  · Walpurga Antl-Weiser²  · Philip R. Nigst^{3,13} 

✉ Marjolein D. Bosch
marjolein.d.bosch@gmail.com

✉ Philip R. Nigst
philip.nigst@univie.ac.at

Stéphane Pirson
stephane.pirson@awap.be

Freddy Damblon
Freddy.Damblon@naturalsciences.be

Margarita Jambrina-Enríquez
mjambri@ull.edu.es

Carolina Mallol
cmallol@ull.edu.es

Alexander Pryor
Alex.Pryor@exeter.ac.uk

William Chase Murphree
wmurphree@ualg.pt

Bence T. Viola
bence.viola@utoronto.ca

Walpurga Antl-Weiser
Walpurga.Antl@nhm.at

¹ Research Group Prehistoric Identities, Department of Prehistory and Western Asia and North African Archaeology, Austrian Archaeological Institute, Austrian Academy of Sciences, Vienna, Austria

² Department of Prehistory, Natural History Museum, Vienna, Austria

³ Human Evolution and Archaeological Sciences (HEAS), University of Vienna, Vienna, Austria

⁴ Agence Wallonne du Patrimoine (AWaP), Service Public de Wallonie, Direction d'appui scientifique et technique, Jambes, Belgium

⁵ European Archaeometry Centre and Department of Geology, University of Liège, Liège, Belgium

⁶ Royal Belgian Institute of Natural Sciences, Brussels, Belgium

⁷ Archaeological Micromorphology and Biomarkers Laboratory, Instituto Universitario de Bio-Orgánica Antonio González, Universidad de La Laguna, San Cristóbal de La Laguna, Santa Cruz de Tenerife, Tenerife, Spain

⁸ Departamento de Biología Animal, Edafología y Geología, Unidad Departamental de Petrología y Geoquímica, Facultad de Ciencias, Universidad de La Laguna, San Cristóbal de La Laguna, Santa Cruz de Tenerife, Tenerife, Spain

⁹ Departamento de Geografía E Historia, Área de Prehistoria (Facultad de Humanidades), Universidad de La Laguna, Campus de Guajara, La Laguna, Santa Cruz de Tenerife, Tenerife, Spain

¹⁰ Department of Archaeology and History, University of Exeter, Exeter, UK

¹¹ Interdisciplinary Center for Archaeology and the Evolution of Human Behavior (ICArEHB), University of Algarve, Faro, Portugal

¹² Department of Anthropology, University of Toronto, Toronto, Canada

¹³ Department of Prehistoric and Historical Archaeology, University of Vienna, Vienna, Austria